PHYSICAL REVIEW D VOLUME 48, NUMBER 8 15 OCTOBER 1993

Neutralino-nucleon scattering reexamined

Manuel Drees
Physics Department, University of Wisconsin, Madison, Wisconsin 53706

Mihoko M. Nojiri
Physics Department, University of Wisconsin, Madison, Wisconsin 53706
and Theory Group, KEK, Oho-machi, Tsukuba, Ibaraki 305, Japan
(Received 6 July 1993)

We present a detailed discussion of the elastic scattering of a supersymmetric neutralino off a nucleon or nucleus, with emphasis on the spin-independent interaction. We carefully treat QCD effects on the squark exchange contribution. In particular, we identify a class of terms that survive even in the absence of mixing in both the neutralino and squark sectors; the corresponding quark and gluon operators also appear in analyses of deep-inelastic lepton-nucleon scattering ("twist-2 operators"), so their hadronic matrix elements are well known. We also reemphasize the importance of mixing between the superpartners of left- and right-handed quarks, and of the contribution from the heavier scalar Higgs boson. We use our refined calculation of the scattering amplitude to update predictions of signal rates for cosmic relic neutralino searches with germanium detectors. In general the counting rate varies strongly with the values (even the signs) of model parameters; typical results lie between a few times 10^{-4} and a few times 10^{-1} events/(kg day).

PACS number(s): 14.80.Ly, 12.10.Dm, 95.30.Cq, 98.80.Cq

I. INTRODUCTION

The lightest supersymmetric particle (LSP) is one of the most attractive candidates for the dark matter (DM) in the Universe [1]. It is theoretically well motivated, since all supersymmetric models [2] with exact "R parity" predict the LSP to be stable. Note that supersymmetry at the weak scale was originally introduced as a solution [3] of the gauge hierarchy problem [4], which has no direct connection to the dark matter problem. It is also worth mentioning that grand unification of the gauge couplings of the standard model (SM) is only compatible [5] with recent precision measurements if additional "light" particles (beyond those present in the SM) exist; the minimal supersymmetric version of the standard model, the MSSM [2], introduces just the right degrees of freedom to allow for grand unification.

In most models, the LSP is the lightest neutralino χ; they therefore automatically satisfy the tight constraints on the cosmic density of stable charged or colored particles that can be derived from unsuccessful searches [6] for exotic isotopes. Moreover, model calculations [7] show that for a wide region of parameter space, the relic density of LSP's left over from the big bang is just large enough to account for the "observed" dark matter or even to allow for a flat universe as favored by inflationary models [1].

Nevertheless, one would like to prove experimentally that some or all of the dark matter is indeed made up from the lightest neutralino χ. Note that even the discovery of some superparticle in a collider experiment will not provide this proof; as far as collider experiments are concerned, the LSP is "stable" if its lifetime exceeds about 10^{-8} sec, while it can only contribute to DM if its lifetime is longer than about 10^{10} yr.

Two methods have been proposed to search for relic neutralinos (or similar particles such as heavy neutrinos). The most direct way is to look for the scattering of ambient DM particles off the nuclei in a detector; experiments using silicon and germanium counters have already reached sufficient sensitivity to exclude massive Dirac neutrinos or sneutrinos as main ingredients of the DM halo of our Galaxy [8]. Alternatively, one can search for energetic neutrinos emerging from the center of the Earth or Sun. The idea here is that a DM particle can lose energy in collisions with nuclei and can then be trapped by the gravitational field of celestial bodies. Eventually, they will become concentrated in the center of these bodies where they will annihilate. Some fraction of these annihilation events will produce energetic (anti)muon neutrinos that can be detected in underground experiments. Currently, the best bounds of this kind come from the Kamiokande group [9]; in the mass range beyond 45 GeV, they are more sensitive to Dirac neutrinos than the counter experiments and even start to impose meaningful bounds on Majorana neutrinos or the lightest neutralino dark matter.

A crucial ingredient in the analysis of both kinds of experiments is a good knowledge of the elastic LSP-nucleus scattering cross section. The counting rate in a direction detection experiment is obviously proportional to this cross section. Since these cross sections determine the rate at which LSP's are captured by the Earth or Sun, they also affect the signal rate in experiments looking for $\chi\chi$ annihilation; in the limiting case where LSP capture by and annihilation in a given celestial body are in equilibrium, the observable neutrino flux is again directly proportional to the LSP-nucleus scattering cross sections.

There are two different kinds of interactions between a neutralino and a nucleon: those that are proportional to

the spin of the nucleus and coherent interactions that are proportional to the nucleon number (or, approximately, mass) of the nucleus. It is important to realize that spin-dependent interactions are not coherent; i.e., the scattering matrix element for heavy nuclei is not enhanced compared to that of single nucleons (apart from trivial phase space factors) and might even be suppressed by nuclear form factors. Nevertheless, the spin-dependent terms are important, since the coherent interactions are often suppressed dynamically, as we will see below. Indeed, early estimates of neutralino nucleus scattering cross sections [10,11] only included the spin-dependent contributions.

However, already Ref. [10] pointed out that a scalar (spin-independent) LSP-quark effective interaction does exist if the quarks are massive. This was first studied quantitatively by Griest [12], using an effective Lagrangian approach in the limit of negligible mixing between the superpartners of left- and right-handed quarks; in this case, a nonzero interaction results only if the LSP is a mixture of gaugino and Higgsino states. Srednicki and Watkins then pointed out [13] that squark mixing introduces additional terms that are generally of the same order as those considered by Griest; these terms survive even if the LSP is a pure gaugino or Higgsino state. Finally, Giudice and Roulet [14] pointed out that Higgs boson exchange also contributes to the coherent LSP-nucleus interactions if the LSP is not a pure state.

The effective interactions studied in Refs. [12–14] all involve massive quarks. In the case of c, b, and t quarks, a coupling to nucleons and nuclei emerges through heavy quark loops coupled to two gluons [15] (see Fig. 1). However, in the case of the squark exchange contribution, this entails the computation of a loop diagram with a (squark) propagator contracted to a point; it is *a priori* not clear under which circumstances this treatment produces a reliable estimate.

In a previous publication [16], we therefore presented a complete one-loop calculation of the neutralino-gluon interaction in the relevant limit of small momentum transfer. We did indeed find contributions that are proportional to the mass of the quark in the loop. We will demonstrate in this paper explicitly that these terms reduce to the results of Refs. [12,13] only if the quark mass is small compared to both the squark and LSP masses, which is frequently not the case for the top quark. We also identified a second class of contributions which are proportional to the LSP mass, not the quark mass; these terms survive even in the absence of mixing in both the neutralino and squark sectors. This is not surprising once one realizes that a coherent interaction is induced by the chiral symmetry breaking of the theory. We also demonstrated that these new terms can be numerically as important as those discussed in Refs. [12–14].

Two problems prevented us from fully exploiting our results in Ref. [16]. On the one hand, we found that the new terms suffered from logarithmic infrared divergences in the limit of vanishing quark mass. On the other hand, our calculation produced terms with gluonic operators different from those encountered in Ref. [15]. We have realized since then that these two seemingly distinct problems actually have a common solution. The new gluonic operator is nothing but a special case of the leading twist gluonic operators encountered in analyses of deep-inelastic lepton-nucleon scattering [17]; the relevant matrix element can be deduced from experimental results. Furthermore, the logarithmic divergence is a consequence of mixing between leading twist quark and gluon operators at the one-loop level. We identified the corresponding quark operators in an expansion of the effective LSP-quark interaction to order $m_{\tilde{q}}^{-4}$. We could then use standard renormalization group techniques to sum the leading logarithms, which are intimately related to "scaling violations" observed in deep-inelastic scattering. This enables us to write down the effective scalar (spin-independent) LSP nucleon interaction including all terms up to order $\alpha_s m_{\tilde{q}}^{-2}$, as well as terms of order $m_{\tilde{q}}^{-4}$, including all leading logarithmic QCD corrections and some nonlogarithmic ("finite") corrections.

The rest of this paper is organized as follows. In Sec. II we present the effective LSP-quark interaction at the tree level, including terms up to order $m_{\tilde{q}}^{-4}$, for the squark exchange contribution. We identify the leading twist quark operator that appears in this order. In Sec. III we discuss QCD effects. We compare the results of Refs. [12,13] with the corresponding results from our full one-loop calculation. We also carefully treat the new terms which survive in the limit of vanishing quark mass, including the twist-2 operators, in a leading logarithmic approximation as well as nonlogarithmic "trace terms." In Sec. IV we present some numerical results for the spin-independent LSP nucleon matrix element. We find that, as anticipated in Ref. [13], squark mixing is usually quite important; however, the treatment of Refs. [12,13] fails in case of the t-quark contribution. We also show some predictions of the counting rate in germanium detectors, where we include the spin-dependent contribution when it is appropriate. Section V is devoted to a brief summary of our main results. Expressions for couplings are listed in Appendix A, while Appendix B contains some loop integrals.

II. EFFECTIVE NEUTRALINO-QUARK INTERACTION

In this section we discuss the effective Lagrangian describing neutralino-quark interactions at the tree level; QCD effects will be discussed in the next section.

Three classes of diagrams contribute to LSP-quark scattering: the exchange of a Z or Higgs boson in the t channel and squark exchange in the s or t channel. As already mentioned in the Introduction, LSP interactions with matter can naturally be separated into spin-dependent and spin-independent parts. Z and squark exchange contribute to the former, and squark and Higgs exchange to the latter. The main interest of this paper is the spin-independent interactions, but for completeness we also list the spin-dependent contribution:

$$\mathcal{L}_{\text{spin}}^{\text{eff}}=\bar{\chi}\gamma^{\mu}\gamma_5\chi\bar{q}\gamma_{\mu}(c_q+d_q\gamma_5)q \ , \tag{1}$$

where we have defined

$$c_q = -\frac{1}{2}\sum_{i=1}^{2}\frac{a_{\tilde{q}_i} b_{\tilde{q}_i}}{m_{\tilde{q}_i}^2 - (m_\chi + m_q)^2} + \frac{g^2}{4m_W^2} O''^R (T_{3q} - 2e_q \sin^2\theta_W) , \tag{2a}$$

$$d_q = \frac{1}{4}\sum_{i=1}^{2}\frac{a_{\tilde{q}_i}^2 + b_{\tilde{q}_i}^2}{m_{\tilde{q}_i}^2 - (m_\chi + m_q)^2} - \frac{g^2}{4m_W^2} O''^R T_{3q} . \tag{2b}$$

The second term in Eqs. (2) describes the Z exchange contribution in the notation of Haber and Kane [2]; g is the SU(2) gauge coupling, θ_W the weak mixing angle, T_{3q} ($=\pm\frac{1}{2}$) and e_q the weak isospin and electric charge of quark q, and O''^R describes the $Z\chi\chi$ coupling [2].

The first term in Eqs. (2) is due to the exchange of the two squarks $\tilde{q}_i$ with a given flavor in the notation of Ref. [16]. The couplings $a_{\tilde{q}_i}$ and $b_{\tilde{q}_i}$ describe scalar and pseudoscalar LSP-quark-squark interactions:

$$\mathcal{L}_{\chi q \tilde{q}} = \sum_{i=1}^{2} \bar{q}(a_{\tilde{q}_i} + b_{\tilde{q}_i}\gamma_5)\chi \tilde{q}_i + \text{H.c.} \tag{3}$$

It is important to realize that $|a_{\tilde{q}_i}| = |b_{\tilde{q}_i}|$ in the chiral limit. In general, these couplings contain both gauge and Yukawa contributions and are sensitive to mixing in both the neutralino and squark sectors. Neutralino mixing has been included in all recent analyses of LSP-nucleus scattering [11–14,18,19], and so we do not describe it again. However, squark mixing has only been taken into account in Ref. [13], and so it might be useful to briefly describe it here.

The mixing between the superpartners of left- and right-handed squarks [20] is determined by the mass matrices [21]

$$\mathcal{M}_{\tilde{u}}^2 = \begin{pmatrix} m_{\tilde{q}_L}^2 + m_u^2 + 0.35 D_Z & -m_u(A_u + \mu\cot\beta) \\ -m_u(A_u + \mu\cot\beta) & m_{\tilde{u}_R}^2 + m_u^2 + 0.16 D_Z \end{pmatrix} , \tag{4a}$$

$$\mathcal{M}_{\tilde{d}}^2 = \begin{pmatrix} m_{\tilde{q}_L}^2 + m_d^2 - 0.42 D_Z & -m_d(A_d + \mu\tan\beta) \\ -m_d(A_d + \mu\tan\beta) & m_{\tilde{d}_R}^2 + m_b^2 - 0.08 D_Z \end{pmatrix} . \tag{4b}$$

Here $D_Z = M_Z^2\cos 2\beta$, with $\tan\beta$ being the usual ratio of vacuum expectation values of the two Higgs doublets, $m_{\tilde{q}_L, \tilde{u}_R, \tilde{d}_R}$ are soft breaking masses, A_u and A_d are soft breaking parameters describing the strength of trilinear scalar interactions, and μ is the supersymmetric Higgs boson (Higgsino) mass parameter that also appears in the neutralino mass matrix. Once squark mixing is included, the mass eigenstates $\tilde{q}_i$ become superpositions of the current eigenstates $\tilde{q}_L, \tilde{q}_R$:

$$\begin{pmatrix} \tilde{q}_1 \\ \tilde{q}_2 \end{pmatrix} = \begin{pmatrix} \cos\theta_q & \sin\theta_q \\ -\sin\theta_q & \cos\theta_q \end{pmatrix} \begin{pmatrix} \tilde{q}_L \\ \tilde{q}_R \end{pmatrix} , \tag{5}$$

with

$$\sin 2\theta_q = \frac{2m_{LR}^2}{m_{\tilde{q}_1}^2 - m_{\tilde{q}_2}^2} , \tag{6}$$

where m_{LR}^2 denotes the (1,2) element of the corresponding mass matrix (4). In the same notation the masses of the squark eigenstates are

$$m_{\tilde{q}_{1,2}}^2 = \tfrac{1}{2}[m_{LL}^2 + m_{RR}^2 \pm \sqrt{(m_{LL}^2 - m_{RR}^2)^2 + 4m_{LR}^4}\,] ; \tag{7}$$

in our convention, $m_{\tilde{q}_1} < m_{\tilde{q}_2}$.

The couplings $a_{\tilde{q}_i}, b_{\tilde{q}_i}$ can now be expressed in terms of the squark mixing angles θ_q and the couplings of squark current eigenstates,

$$a_{\tilde{q}_1} = \tfrac{1}{2}[\cos\theta_q(X_{q0} + Z_{q0}) + \sin\theta_q(Y_{q0} + Z_{q0})] , \tag{8a}$$

$$b_{\tilde{q}_1} = \tfrac{1}{2}[\cos\theta_q(X_{q0} - Z_{q0}) + \sin\theta_q(Z_{q0} - Y_{q0})] , \tag{8b}$$

where we have used the notation of Ref. [22]:

$$X_{q0} = -\sqrt{2}g[T_{3q}N_{02} - \tan\theta_W(T_{3q} - e_q)N_{01}] , \tag{9a}$$

$$Y_{q0} = \sqrt{2}g\tan\theta_W e_q N_{01} , \tag{9b}$$

$$Z_{u0} = -\frac{g m_u N_{04}}{\sqrt{2}\sin\beta m_W} , \quad Z_{d0} = -\frac{g m_d N_{03}}{\sqrt{2}\cos\beta m_W} . \tag{9c}$$

In terms of the parameters a, b, c of Griest [12], one has $X_{q0} = -\sqrt{2}gb$, $Y_{q0} = \sqrt{2}gc$, and $Z_{q0} = -\sqrt{2}ga$. The couplings $a_{\tilde{q}_2}, b_{\tilde{q}_2}$ of the heavier squark eigenstate can be obtained from Eqs. (8) by the transformation $\sin\theta_q \to \cos\theta_q$, $\cos\theta_q \to -\sin\theta_q$ [see Eq. (5)].

Recall that χ is a Majorana particle; the vertices one reads off the effective Lagrangian (1) thus have to be multiplied by 2. Note that we have included the LSP and quark masses in our quark propagator; this propagator therefore accurately describes the scattering of a massive LSP off a massive quark in the limit where the momentum transfer is negligible. Since ambient LSP's are expected [1] to have velocities $v \simeq 10^{-3}c$, this approximation is justified.

Except for our refined propagator, our effective Lagrangian (1) agrees with Griest's [12] up to a factor 2 in the limit $\theta_q \to 0$.[1] In the same limit we agree with Ellis and Flores [18] except for the relative sign between the Z and $\tilde{q}$ exchange terms. In the limit of small but nonzero squark mixing, we reproduce the result of Ref. [13] for the squark exchange contribution in the limit $m_{\tilde{q}_i}^2 \gg (m_q + m_\chi)^2$.

We finally mention that the contribution from the quark vector current, described by c_q, to the LSP-nucleon scattering matrix element is suppressed by a factor of the LSP velocity v and is therefore negligible in practice; we have included it here to allow comparison with results in the literature [12,13,18]. We have, however, omitted squark exchange contributions

[1] We agree with his expression for the cross section.

$$\sim(a_{\tilde{q}_i}^2-b_{\tilde{q}_i}^2)/[m_{\tilde{q}_i}^2-(m_q+m_\chi)^2]^2 ,$$

since they are doubly suppressed compared to the leading terms given in Eqs. (2): The coupling is nonzero only due to chirality violation, which is generally weak; moreover, this contribution is of higher order in an expansion in inverse powers of the squark mass.

We now turn to the spin-independent neutralino-quark interactions. They receive contributions from the exchange of squarks and scalar Higgs bosons:

$$\mathcal{L}_{\text{spin,indep}}^{\text{eff}}=f_q\bar{\chi}\chi\bar{q}q+g_q\bar{\chi}\gamma^\mu\partial^\nu\chi(\bar{q}\gamma_\mu\partial_\nu q-\partial_\nu\bar{q}\gamma_\mu q) . \tag{10}$$

Here we have introduced

$$f_q=-\frac{1}{4}\sum_{i=1}^{2}\frac{a_{\tilde{q}_i}^2-b_{\tilde{q}_i}^2}{m_{\tilde{q}_i}^2-(m_\chi+m_q)^2}+m_q\sum_{j=1}^{2}\frac{c_\chi^{(j)}c_q^{(j)}}{m_{H_j}^2} , \tag{11a}$$

$$g_q=-\frac{1}{4}\frac{a_{\tilde{q}_i}^2+b_{\tilde{q}_i}^2}{[m_{\tilde{q}_i}^2-(m_\chi+m_q)^2]^2} . \tag{11b}$$

The couplings $a_{\tilde{q}_i},b_{\tilde{q}_i}$ entering the squark exchange contributions are again given by Eqs. (8). The coefficients $c_\chi^{(j)}$ and $c_q^{(j)}$ determine the couplings of the jth scalar Higgs boson to the LSP and to the quark q, respectively [16]; for the convenience of the reader, explicit expression are given in Appendix A.

Only the term $\propto f_q$ has been discussed in the existing literature. In the limit $\theta_q\to 0$, our expression (11a) agrees with Ellis and Flores [18] (up to an overall sign). The Higgs boson exchange contribution to f_q agrees with Ref. [14], where the importance of this term was first pointed out; however, here as well as in Refs. [18] and [23] only the contribution from the light Higgs boson H_2 has been taken into account. As first pointed out in Ref. [19], the contribution of the heavier Higgs boson H_1 can also be very important, since its coupling to quarks can be enhanced.[2] However, the squark exchange contribution in Ref. [19] is too large by a factor of 2. Moreover, unlike in Refs. [19] and [23], the relative sign between the Higgs boson and squark exchange terms should not depend on the sign of the eigenvalue m_χ of the neutralino mass matrix. Finally, our squark exchange contribution (11a) agrees with Ref. [13] in the limit of small but nonzero squark mixing.

Note that the squark exchange contribution to Eq. (11a) is proportional to the difference $a_{\tilde{q}_i}^2-b_{\tilde{q}_i}^2$, which vanishes in the limit of a chiral LSP-quark-squark interaction. Indeed, Eqs. (4)–(9) imply that this coefficient vanishes for massless quarks: From Eqs. (8) and (9), we see that $a_{\tilde{q}_i}^2-b_{\tilde{q}_i}^2\propto\sin 2\theta_q$ for massless quarks ($Z_{q0}=0$); on the other hand, from Eq. (6) one has $\sin 2\theta_q\propto m_q/m_{\tilde{q}}$. We thus conclude that $q_{\tilde{q}_i}^2-b_{\tilde{q}_i}^2$ is very small for the light quarks that are abundant in nucleons. Heavy quarks couple to nucleons only through a loop; this will be discussed in the next section. Since the $O(m_{\tilde{q}}^{-2})$ term is suppressed, the contribution from g_q can be important, even though it is $O(m_{\tilde{q}}^{-4})$. For the interesting case of a b-ino-like LSP, $a_{\tilde{q}_i}^2+b_{\tilde{q}_i}^2$ is of the order of the squared U(1) gauge coupling, without any suppression from small mixing angles. If the LSP is Higgsino-like, the coupling to light quarks is suppressed, but this scenario is cosmologically not very interesting, since the relic density of Higgsino-like states is very small [7,22,24].

In order to compute LSP-nucleus scattering cross sections from Eq. (10), we have to know the nucleonic matrix elements of the relevant quark operators. For light (u,d,s) quarks the matrix elements $\langle N|m_q\bar{q}q|N\rangle$ have to be taken from calculations that attempt to describe strong interactions at long distances. Following Refs. [19,23], we will use results from chiral perturbation theory as a guideline [25]. The matrix elements $\langle N|m_Q\bar{Q}Q|N\rangle$ for heavy (c,b,t) quarks can be computed as in Ref. [15] (see Sec. 3). Finally, the second term in the effective Lagrangian (10) can be expressed in terms of twist-2 quark operators that appear in analyses of deep-inelastic lepton-nucleon scattering [17]. This can be seen using the tensor identity

$$Q_{\mu\nu}L^{\mu\nu}=(Q_{\mu\nu}-\tfrac{1}{4}g_{\mu\nu}Q_\alpha^\alpha)L^{\mu\nu}+\tfrac{1}{4}Q_\alpha^\alpha L_\beta^\beta , \tag{12}$$

as well as the equation of motion for the "trace terms" $\bar{q}\gamma^\mu\partial_\mu q$ and $\bar{\chi}\gamma^\nu\partial_\nu\chi$, to rewrite the second term in Eq. (10) as

$$\mathcal{L}_{m_{\tilde{q}}^{-4}}^{\text{eff}}=g_q[-2i\mathcal{O}_{q\mu\nu}^{(2)}\bar{\chi}\gamma^\mu\partial^\nu\chi-\tfrac{1}{2}m_q m_\chi\bar{q}q\bar{\chi}\chi] . \tag{13}$$

Here we have introduced the $n=2$ twist-2 quark operator [17]

$$\mathcal{O}_{q\mu\nu}^{(2)}=\frac{i}{2}[\bar{q}\gamma_\mu\partial_\nu q+\bar{q}\gamma_\nu\partial_\mu q-\tfrac{1}{2}\bar{q}\partial_\alpha\gamma^\alpha q g_{\mu\nu}] . \tag{14}$$

Note that $\mathcal{O}_{q\mu\nu}^{(2)}$ is traceless, which is necessary for operators with fixed spin or "twist."

The characteristic energy scale for the effective Lagrangian (10) is given by the Higgs boson and squark propagators. In order to describe physics at lower scales, QCD renormalization effects must be included. These are the subject of the following section.

III. QCD EFFECTS ON LSP-NUCLEON SCATTERING

In this section we discuss the role QCD plays in calculating the LSP-nucleon scattering matrix element. Two independent effects have to be considered. On the one hand, perturbative QCD predicts a nonzero matrix element $\langle N|m_Q\bar{Q}Q|N\rangle$ for heavy quarks [15]. On the other hand, QCD also changes the coefficient g_q of the twist-2 operator appearing in the effective Lagrangian (10).

We start with a discussion of the heavy quark contribution. It has been realized more than 15 years ago that

[2]The expression for the $H_1\chi\chi$ coupling in Ref. [19] contains a sign mistake; M. Kamionkowski (private communication).

a scalar heavy quark current couples to nucleons with strength $\sim 1/m_Q$ via the loop diagram depicted in Fig. 1. The result is [15,25]

$$\langle N|m_Q\bar{Q}Q|N\rangle = \tfrac{2}{27} m_N \left[1 - \sum_{u,d,s} f_{Tq}\right] \quad (Q=c,b,t) \ . \tag{15}$$

Here f_{Tq} denotes the fraction of the nucleon mass m_N that is due to light quark q:

$$\langle N|m_q\bar{q}q|N\rangle = m_N f_{Tq} \quad (q=u,d,s) \ . \tag{16}$$

The numerical values of the f_{Tq} have to be taken from model calculations [25], as mentioned earlier.

Equation (15) describes the Higgs boson exchange contribution exactly (up to corrections of order of the momentum transfer divided by m_Q); indeed, it has first been derived [15] in a calculation of the Higgs-boson–nucleon coupling. However, when applying Eq. (15) to the squark exchange contribution, one effectively replaces a box diagram with one squark and three quark propagators by a triangle diagram that only contains quark propagators. This procedure cannot be expected to yield accurate results unless $m_{\tilde{q}}^2 \gg (m_q + m_\chi)^2$. This is frequently not the case for top squarks and can also be problematic for the bottom squark, as we will see later.

In Ref. [16] we therefore presented a full one-loop calculation of the contribution from heavy quarks and their superpartners. This also includes the contributions of box and triangle diagrams with two or three squark propagators; indeed, these diagrams are necessary to guarantee gauge invariance to all orders in $m_q/m_{\tilde{q}}$. As mentioned above, the Higgs boson coupling to nucleons via a heavy quark loop is given exactly by Eq. (15); however, there is also a contribution involving only the superpartners of heavy quarks. The total contribution involving squarks can be described by the following effective

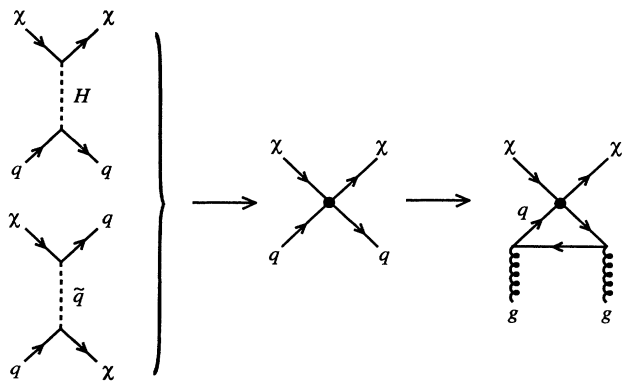

FIG. 1. On the left we depict the Feynman diagrams that contribute to spin-independent LSP-quark interactions. In the low-energy limit and after a Fierz rearrangement of the $\tilde{q}$ exchange contribution, these give rise to the effective interaction depicted in the center. In previous work the contribution involving c,b,t quarks has been estimated closing the quark line as shown in the diagram at the right.

LSP gluon interaction[3] [16]:

$$\begin{aligned}\mathcal{L}_{\chi g}^{\text{eff}} = \bar{\chi}\chi F^a_{\mu\nu}F^{a\mu\nu}[-T_{\tilde{q}} + B_D + B_S] \\ -(B_{1D}+B_{1S})\bar{\chi}\partial_\mu\partial_\nu\chi F^{a\mu\rho}F^{a\nu}_\rho \\ +B_{2S}\bar{\chi}(i\partial_\mu\gamma_\nu + i\partial_\nu\gamma_\mu)\chi F^{a\mu\rho}F^{a\nu}_\rho \ .\end{aligned} \tag{17}$$

Here $T_{\tilde{q}}$ is the Higgs contribution via squark loops, while all other contributions come from box and triangle diagrams involving quarks and squarks. All coefficients with a subscript D are proportional to the difference $a_{\tilde{q}_i}^2 - b_{\tilde{q}_i}^2$ (summed over quarks and squarks), while a subscript S indicates a contribution proportional to $q_{\tilde{q}_i}^2 + b_{\tilde{q}_i}^2$:

$$B_D = \frac{\alpha_S}{4\pi}\frac{1}{8}\sum_{q,i}(a_{\tilde{q}_i}^2 - b_{\tilde{q}_i}^2) m_q I_1(m_{\tilde{q}}, m_q, m_\chi) \ , \tag{18a}$$

$$B_S = \frac{\alpha_S}{4\pi}\frac{1}{8} m_\chi \sum_{q,i}(a_{\tilde{q}_i}^2 + b_{\tilde{q}_i}^2) I_2(m_{\tilde{q}}, m_q, m_\chi) \ , \tag{18b}$$

$$B_{1D} = \frac{\alpha_S}{4\pi}\frac{1}{3}\sum_{q,i}(a_{\tilde{q}_i}^2 - b_{\tilde{q}_i}^2) m_q I_3(m_{\tilde{q}}, m_q, m_\chi) \ , \tag{18c}$$

$$B_{1S} = \frac{\alpha_S}{4\pi}\frac{1}{3} m_\chi \sum_{q,i}(a_{\tilde{q}_i}^2 + b_{\tilde{q}_i}^2) I_4(m_{\tilde{q}}, m_q, m_\chi) \ , \tag{18d}$$

$$B_{2S} = \frac{\alpha_S}{4\pi}\frac{1}{12}\sum_{q,i}(a_{\tilde{q}_i}^2 + b_{\tilde{q}_i}^2) I_5(m_{\tilde{q}}, m_q, m_\chi) \ , \tag{18e}$$

$$T_{\tilde{q}} = \frac{\alpha_S}{4\pi}\frac{1}{24}\sum_{j=1}^{2}\frac{c_\chi^{(j)}}{m_{H_j}^2}\sum_{q,i}\frac{c_{\tilde{q}_i}^{(j)}}{m_{\tilde{q}_i}^2} \ . \tag{18f}$$

Expressions for the couplings appearing in Eq. (18f) are given in Appendix A, while the loop integrals in Eqs. (18a)–(18e) are listed in Appendix B.

The effective Lagrangian (17) contains terms with different tensor structure. The matrix element (15) is related to the "trace term" $F^a_{\mu\nu}F^{a\mu\nu}$, while the terms $\propto F^{a\mu\rho}F^{a\nu}_\rho$ are related to the twist-2 operator. We will discuss these two kinds of terms in the following subsections.

A. Trace part

We start with the contribution $\propto F^a_{\mu\nu}F^{a\mu\nu}$, which corresponds to the contribution described by Eq. (15). It is important to realize that we have to include the trace part of the terms $\propto B_1$ and B_2 here; i.e., we have to apply the tensor identity (12) to these terms. The total "trace term" then becomes

$$\mathcal{L}_{\chi g,\text{trace}}^{\text{eff}} = \bar{\chi}\chi F^a_{\mu\nu}F^{a\mu\nu}\left[-T_{\tilde{q}} + B_D + B_S - \frac{m_\chi}{2}B_{2S} - \frac{m_\chi^2}{4}(B_{1D}+B_{1S})\right] \ . \tag{19}$$

[3]Note that the signs of the terms proportional to T_q, $T_{\tilde{q}}$, B_{1S}, and B_{1D} were incorrect in our original calculation.

In order to compare Eq. (19) with the result one obtains from using Eq. (15) on *all* terms $\sim m_Q \bar{Q}Q$ in the effective Lagrangian (10), we use the identity [15,25]

$$\frac{\alpha_S}{4\pi}\langle N|F^a_{\mu\nu}F^{a\mu\nu}|N\rangle = -\tfrac{2}{9}m_N\left[1-\sum_{u,d,s} f_{Tq}\right] . \quad (20)$$

Moreover, we need the expansion of the loop integrals I_{1-5} in powers of inverse squark mass, i.e., for the case $m_q^2 \ll m_{\tilde{q}}^2 - m_\chi^2$:

$$I_1 \simeq \frac{2}{3m_q^2(m_{\tilde{q}}^2-m_\chi^2)} + O\left[\frac{1}{m_{\tilde{q}}^4}\right] , \quad (21a)$$

$$I_2 - \frac{1}{3}I_5 \simeq -\frac{2}{3m_{\tilde{q}}^4} + O\left[\frac{m_\chi^2}{m_{\tilde{q}}^6}, \frac{m_q^2}{m_{\tilde{q}}^6}\right] , \quad (21b)$$

$$I_3, I_4 \simeq O\left[\frac{1}{m_{\tilde{q}}^6}\right] . \quad (21c)$$

We see that Eqs. (18)–(21a) give the *same* result to leading order in $m_{\tilde{q}}^{-2}$ as the squark exchange contribution (11a) to the effective Lagrangian (10) when used together with Eq. (15). However, Eq. (21b) gives a 2 times *larger* result than Eqs. (11b) and (13) when used together with Eq. (15). This illustrates the perils of using effective Lagrangians in loop calculations. Such a procedure can only be expected to give the correct answer if the loop integration is dominated by momenta small compared to the squark mass. In the limit $m_q \ll m_{\tilde{q}}$, this is true for I_1, which has a quadratic infrared (IR) singularity as $m_q \to 0$. We will see below that this is also true for I_2 and I_5 separately, which show logarithmic IR divergences as $m_q \to 0$. However, these singularities cancel in the relevant combination $I_2 - \frac{1}{3}I_5$. In other words, in this particular combination loop momenta of the order of the squark mass make significant contributions. The effective Lagrangian approach corresponds to introducing a cutoff of the order of the squark mass on the loop integration; it is clear that this cannot yield reliable results if loop momenta close to the cutoff contribute significantly.

We thus conclude that the effective Lagrangian approach that has been used in the literature to estimate the heavy (c,b,t) quark contribution to LSP-nucleon scattering from the first term in Eq. (10) should give approximately the correct result if $m_q^2 \ll m_{\tilde{q}}^2 - m_\chi^2$. However, the heavy quark contribution from the second term in Eq. (10) *cannot* be estimated in this fashion; one has to use the results of the full one-loop calculation.

The contributions from B_D and B_S differ also where light (u,d,s) quarks are concerned. As discussed earlier, their contribution from the effective Lagrangians (10) and (13) has to be estimated using model calculations [25] for $\langle N|m_q\bar{q}q|N\rangle$. It does not make sense to include the light quark contribution to B_D, since the corresponding loop integral I_2 is dominated by the nonperturbative region of small momenta; this effect should be included in the nonperturbative nucleonic matrix elements. On the other hand, the light quark contribution to $B_S - (m_\chi/2)B_{2S}$ *can* safely be included, since here the relevant loop integral is dominated by the perturbative region of large momenta, which is not included in the matrix elements of $m_q\bar{q}q$. Another way to see that these two contributions are indeed independent and can thus safely be added is the observation that in Eq. (13) chirality is violated by the quark mass, while in $B_S - (m_\chi/2)B_{2S}$ the LSP mass provides the source of chirality breaking.

B. Contributions from twist-2 operators

We now turn to a discussion of QCD effects on the twist-2 quark operator (14) in the effective Lagrangian (13). As mentioned at the end of Sec. II, the effective Lagrangian describes physics at the energy scale given by the squark propagator. In more formal language we have to know the matrix element $\langle N|\mathcal{O}^{(2)}_{q\mu\nu}|N\rangle$ at the renormalization point $\mu_0 = \sqrt{m_{\tilde{q}}^2 - m_\chi^2}$ in order to directly use Eq. (13). This matrix element is closely related to the second moment of the quark distribution functions [17]:

$$\langle N|\mathcal{O}^{(2)}_{q\mu\nu}|N\rangle|_{\mu_0} = \frac{1}{m_N}(p_\mu p_\nu - \tfrac{1}{4}m_N^2 g_{\mu\nu})\int_0^1 dx\, x[q(x,\mu_0^2)+\bar{q}(x,\mu_0^2)] , \quad (22)$$

where p is the nucleon momentum.[4]

In principle, we could use Eq. (22) directly. However, this has the practical disadvantage that the hadronic matrix elements would depend on supersymmetric (SUSY) parameters via the scale dependence of the parton distribution functions (these are the famous scaling violations of QCD). We therefore choose to express our results in terms of matrix elements of twist-2 operators at the fixed (low) scale $Q_0 = 5$ GeV $(\simeq m_b)$. The moments of parton densities at high momentum scales are related to those at a lower scale via the renormalization group equations [17]

$$\frac{d}{d\ln Q}q(n,Q^2) = -[\gamma^F_{FF}(n)q(n,Q^2)+\gamma^F_{FV}(n)G(n,Q^2)] , \quad (23a)$$

$$\frac{d}{d\ln Q}G(n,Q^2) = -\left[\gamma^V_{FF}(n)\sum_q q(n,Q^2)+\gamma^V_{FV}(n)G(n,Q^2)\right] , \quad (23b)$$

where we have introduced

$$q(n,Q^2) \equiv \int_0^1 dx\, x^{n-1}q(x,Q^2) \quad (24)$$

and similarly for $G(n,Q^2)$. Note that the sum in Eq. (23b) runs over all quarks and antiquarks whose mass is (much) smaller than Q. The $\gamma^i_{jj}(n)$ are components of a 2×2 matrix of anomalous dimensions [17].

[4]Recall that we assume negligible momentum transfer, so that the initial and final momenta are identical.

In order to solve Eqs. (23), we first observe that flavor nonsinglet operators $q_i(n,Q^2)-q_j(n,Q^2)$, where i,j are flavor indices, renormalize multiplicatively, since the gluonic contribution in Eq. (23a) cancels out. It is always possible to express l independent quark densities in terms of $l-1$ differences and the total sum $\Sigma(n,Q^2) \equiv \sum_{\text{quarks}} q(n,Q^2)$. Finally, in order to treat the mixing between $\Sigma(n)$ and $G(n)$, one introduces orthogonal combinations $\mathcal{O}_+(n)$ and $\mathcal{O}_-(n)$, which again renormalize multiplicatively with anomalous dimensions $\gamma_+(n)$ and $\gamma_-(n)$. For the relevant case $n=2$ and $N_f=5$ light flavors of quarks, these operators are given by [17]

$$\mathcal{O}_+(2,Q^2)=\tfrac{16}{31}\Sigma(2,Q^2)-\tfrac{15}{31}G(2,Q^2) , \tag{25a}$$

$$\mathcal{O}_-(2,Q^2)=\tfrac{15}{31}[\Sigma(2,Q^2)+G(2,Q^2)] , \tag{25b}$$

while the relevant anomalous dimensions are

$$\gamma_{FF}^F(2)=\frac{16\alpha_S}{9\pi} , \quad \gamma_+(2)=\frac{31\alpha_S}{9\pi} , \quad \gamma_-(2)=0 . \tag{26}$$

Note that the second moment of a parton density is nothing but the fraction of the total nucleon momentum carried by that species of partons. The sum over all quarks and gluons $\Sigma(2)+G(2)$ must therefore be equal to 1 at all momentum scales. This explains why $\gamma_-(2)$ vanishes. We thus succeeded in reducing the system of coupled equations (23) to decoupled equations of the form

$$\frac{d}{d\ln Q}\mathcal{O}(Q^2)=-\frac{\alpha_S}{\pi}\bar{\gamma}\mathcal{O}(Q^2) , \tag{27}$$

which has the solution [17] (for $N_f=5$ flavors)

$$\mathcal{O}(Q^2)=\mathcal{O}(Q_0^2)\left[\frac{\alpha_S(Q^2)}{\alpha_S(Q_0^2)}\right]^{6\bar{\gamma}/23} . \tag{28}$$

Here we have used the standard expression for the running QCD coupling constant:

$$\alpha_S(Q^2)=\frac{12\pi}{23\ln(Q^2/\Lambda^2)} . \tag{29}$$

In order to apply Eqs. (23)–(29) to our problem, we first observe that we can safely ignore the Yukawa contributions to the combinations of couplings $a_{\tilde{q}_i}^2+b_{\tilde{q}_i}^2$ for u, d, s, and c (s)quarks. If we further assume that squarks of the first two generations are degenerate in mass, as suggested by the analysis of SUSY contributions to meson mixing in the K^0 and B^0 systems [26], we find that the coefficients g_q are equal for u and c quarks and for d and s quarks. On the other hand, for large $\tan\beta$ the bottom Yukawa coupling can be sizable; moreover, if $\tan\beta$ and/or μ are large, Eq. (4b) leads to non-negligible mass splitting between bottom squarks. In general, g_b can therefore differ significantly from $g_d=g_s$. Altogether, we therefore need three independent combinations of quark densities for five quarks (the contribution of the top quark will be discussed later):

$$\sum_{\text{quarks}} g_q q(Q^2)=\tfrac{1}{5}(2g_u+2g_d+g_b)[\mathcal{O}_+(Q^2)+\mathcal{O}_-(Q^2)]+\tfrac{1}{2}(g_u-g_d)[\mathcal{O}_u(Q^2)-\mathcal{O}_d(Q^2)]$$
$$+\tfrac{1}{5}(g_u+g_d-2g_b)[\tfrac{1}{2}\Sigma(Q^2)-5b(Q^2)] . \tag{30}$$

Here we have used Eqs. (25) to replace the sum over quark densities Σ by the orthogonal combinations $\mathcal{O}_+$ and $\mathcal{O}_-$. Moreover, we have made the usual assumption that $q(x)=\bar{q}(x)$ for the s, c, and b quark densities in nucleons and have introduced

$$\mathcal{O}_u=u+\bar{u}+2c, \quad \mathcal{O}_d=d+\bar{d}+2s . \tag{31}$$

Equation (30) holds at any scale Q^2. As discussed earlier, we have to evaluate it at the high scale $\mu_0^2=m_{\tilde{q}}^2-m_\chi^2$, but we want to express the result in terms of parton densities at fixed scale $Q_0^2=25\ \text{GeV}^2\simeq m_b^2$; this scale has been chosen such that $b(Q_0^2)=0$.[5] Using Eqs. (26)–(28), we have

$$\sum_{\text{quarks}} g_q q(\mu_0^2)=\tfrac{1}{5}(2g_u+2g_d+g_b)\left[\frac{15}{31}+\mathcal{O}_+(Q_0^2)\left[\frac{\alpha_S(\mu_0^2)}{\alpha_S(Q_0^2)}\right]^{62/69}\right]$$
$$+\{\tfrac{1}{2}(g_u-g_d)[\mathcal{O}_u(Q_0^2)-\mathcal{O}_d(Q_0^2)]+\tfrac{1}{10}(g_u+g_d-2g_b)\Sigma(Q_0^2)\}\left[\frac{\alpha_S(\mu_0^2)}{\alpha_S(Q_0^2)}\right]^{32/69} , \tag{32}$$

where we have used momentum conservation, which implies $\mathcal{O}_-(2)=\frac{15}{31}$ as discussed above. The other necessary combinations of moments of parton densities at scale Q_0^2 can easily be obtained by integrating standard parametrizations of these densities. Results for four recent representative parametrizations [27,28] are collected in Table I.

Equation (32) describes our results in terms of constant parameters g_q of the effective Lagrangian and scale-dependent hadronic matrix elements. Equivalently, we could have used running couplings and constant matrix elements. The crucial observation here is that the product $g_q(Q^2)q(Q^2)$ is *independent* of the scale Q^2.

[5] Nevertheless, the last term in Eq. (30) renormalizes multiplicatively, like any other nonsinglet quark density, since $b(Q^2)$ is nonzero for $Q^2>Q_0^2$.

TABLE I. Numerical values of the second moments of the combinations of parton densities appearing in Eq. (32). "MTLO", "MTB1", and "MTB2" refer to the leading-order parametrization and two next-to-leading-order parametrizations of Morfin and Tung [27], where we have set $b(Q_0^2)\equiv 0$ exactly, while "Owens" refers to the parametrization of Ref. [28]. Columns 2–5 refer to scale $Q_0^2\simeq m_b^2$, while column 6 gives the gluon density at scale $Q^2=2\times 10^4$ GeV$^2\simeq m_t^2$. The superscripts in columns 3 and 4 refer to the proton and neutron; the other entries are identical for both kinds of nucleon.

	$\mathcal{O}_+$	$\mathcal{O}_u^p-\mathcal{O}_d^p$	$\mathcal{O}_u^n-\mathcal{O}_d^n$	Σ	G
MTB1	0.025	0.115	−0.181	0.509	0.492
MTB2	0.056	0.102	−0.190	0.540	0.471
MTLO	0.019	0.113	−0.181	0.503	0.480
Owens	0.018	0.109	−0.171	0.502	0.514

Note that Eq. (32) depends on the gluon density at scale Q_0^2. This dependence is entirely due to the scale dependence of the parton densities, which in turn is induced by QCD loops. If we expand Eq. (32) in α_S, keeping only terms linear in α_S, the coefficient of $G(Q_0^2)$ on the right-hand side of Eq. (32) is $(\alpha_S/3\pi)\ln(\mu_0/Q_0)\sum g_q$. On the other hand, the traceless part of the combination of gluon field strength in the second and third terms in the effective Lagrangian (17) is nothing but the $n=2$ twist-2 gluon operator:

$$\langle N|F^{a\mu\rho}F_\rho^{a\nu}+\tfrac{1}{4}g^{\mu\nu}F^a_{\alpha\beta}F^{a\alpha\beta}|N\rangle = \frac{1}{m_N}(p^\mu p^\nu - m_N^2 g^{\mu\nu})G(2)\ . \quad (33)$$

Moreover, in the limit $m_q\to 0$, the coefficient B_{2S} contains a logarithmic divergence:

$$B_{2S}\simeq\frac{\alpha_S}{4\pi}\frac{1}{6}\sum_{q,i}\frac{a_{\tilde q_i}^2+b_{\tilde q_i}^2}{(m_{\tilde q_i}^2-m_\chi^2)^2}\ln\frac{m_{\tilde q_i}^2-m_\chi^2}{m_q^2}+\text{finite terms}$$
$$=-\frac{\alpha_S}{3\pi}\ln\frac{\mu_0}{m_q}\sum g_q\ ; \quad (34)$$

in the second step, we have assumed squarks to be (essentially) degenerate, as for the discussion leading to Eq. (32). The renormalization group analysis thus exactly reproduces the leading logarithmic contribution to the full one-loop amplitude[6] if we identify Q_0 with the quark mass m_q. This is no surprise; in the given case, the loop integral is again dominated by small loop momenta, leading to an IR divergence as $m_q\to 0$, and so we expect the effective Lagrangian approach to (approximately) reproduce the one-loop result.

For the case of light (u,d,s) quarks, we cannot trust the one-loop calculation, since their masses are so small that perturbative QCD is no longer trustworthy at scales $Q\simeq m_q$. Nonperturbative effects become important, which are included in the (measured) parton distribution functions. The light quarks therefore have to be treated using the effective Lagrangians (13) and (32).

On the other hand, for heavy (c,b,t) quarks the perturbative result of Eqs. (17) and (18) should be reliable to the given (one-loop) order. Nevertheless, the use of the renormalization group equation (RGE) approach [Eq. (32)] might be advantageous, since it automatically sums leading logarithmic QCD corrections to all orders [17], i.e., all terms $\sim[\alpha_S\ln(\mu_0/m_q)]^n$ are included. For the case of c quarks, we find that the logarithmic term does indeed dominate the loop integral I_5. Summing higher powers of this logarithm is therefore quite important; we thus decided to treat c quarks in the RGE approach. In case of the top quark, the logarithmic term in I_5 dominates only if the top squark is very heavy, in which case the total contribution $\sim g_t$ is very small anyway. It therefore appears more important to include nonlogarithmic terms rather than resumming higher powers of the logarithm. We thus treat the t-quark contribution in exact one-loop order using Eqs. (17), (18), and (33), where we take the gluon density at scale[7] $Q^2=2\times 10^4$ GeV$^2\simeq m_t^2$.

The case of the (s)bottom contribution is somewhat more ambiguous. For small $\tan\beta$, $\tilde b$ squarks are usually degenerate with the other squarks, and I_5 is dominated by the logarithmic term. However, for large $\tan\beta$ the lighter bottom squark eigenstate can be much lighter than the other squarks and can even be close in mass to the LSP. In this case the exact one-loop treatment seems more appropriate. In particular, I_5 remains finite as $m_{\tilde b_1}\to m_\chi$ or $m_{\tilde b_1}\to m_\chi+m_b$, while the coefficient g_b diverges in this limit. We therefore decided to treat the (small) contribution from the heavier bottom squark $\tilde b_2$ together with the squarks of the first two generations via Eq. (32). In order to include the contribution from $\tilde b_1$ exchange, we introduce a new scale $\mu_b^2=m_{\tilde b_1}^2-m_\chi^2$; as discussed above, this scale can be significantly smaller than μ_0^2. We then compare the $\tilde b_1$ exchange contribution according to Eqs. (17) and (18) with the prediction from the RGE approach and adopt the *smaller* of the two results as our best estimate. Since the terms of higher order in

[6]Recall that the twist-2 quark operators appear with coefficient -2 in the effective Lagrangian (13), while the term $\propto B_{2S}$ in Eq. (17) gets a factor of 2 since we have used the explicitly symmetric form of the LSP tensor following the notation of Ref. [16].

[7]At high momentum scale $G(n,Q^2)$ depends only very weakly on Q^2. The use of a fixed Q^2 is therefore justified for top quark mass in the allowed range between 100 and 200 GeV.

$\ln(\mu_b/Q_0)$ tend to reduce the one-loop result, this procedure implies that we treat the $\tilde{b}_1$ contribution via the RGE method if $\tilde{b}_1$ is heavy. However, close to the spurious pole in g_b the RGE prediction diverges, and our procedure automatically chooses the one-loop result.

This completes our treatment of QCD effects. We now turn to a discussion of the numerical importance of the various contributions to LSP-nucleon scattering.

IV. NUMERICAL RESULTS

A. LSP-nucleon scattering amplitude

Before we can give numerical results for LSP-nucleon scattering amplitudes, we have to specify the values of some parameters. As already mentioned in the previous section, recent predictions [27,28] for the second moments of the relevant combination of parton densities are listed in Table I. We see that existing data on deep-inelastic lepton-nucleon scattering and related data which enter the fits of Refs. [27,28] are sufficient to pin down these parameters to better than 10% accuracy.

We also need to specify the values of $f_{Tq} \equiv \langle N|m_q\bar{q}q|N\rangle/m_N$ for light (u,d,s) quarks. The contributions from u and d quarks is quite small, but we include them for completeness. The combination $(m_u+m_d)/2\langle N|\bar{u}u+\bar{d}d|N\rangle$ is determined from the πN "sigma term." However, since u and d quarks couple differently, we have to know the individual contributions, which are more model dependent. Following Cheng [25], we take

$$f_{Tu}^{(p)}=0.023\ ,\quad f_{Td}^{(p)}=0.034\ ,$$
$$f_{Tu}^{(n)}=0.019\ ,\quad f_{Td}^{(n)}=0.041\ , \tag{35}$$

where the superscripts denote protons p and neutrons n.

The strange quark contribution is expected to be larger than that from u and d quarks, but the exact value is quite uncertain. Values as small as 71 MeV [29] and as high as 430 MeV [25] have been given for the matrix element $\langle N|m_s\bar{s}s|N\rangle$. Here we follow the recent analysis of Gasser, Leutwyler, and Sainio [30]:

$$f_{Ts}=0.14\ ; \tag{36}$$

it should be kept in mind that this value is uncertain to about a factor of 2, however.

In order to estimate the contribution from the spin-dependent interactions of Eqs. (1) and (2), we have to know the matrix elements

$$\langle N|\bar{q}\gamma_\mu\gamma_5 q|N\rangle = 2s_\mu\Delta q\ . \tag{37}$$

Here s_μ is the spin vector of the nucleon and Δq denotes the second moment of the polarized quark density [31]. Just like the unpolarized parton densities, the Δq can be extracted from analyses of deep-inelastic lepton-nucleon scattering. However, in this case both probe and target have to be polarized, which complicates the experiments significantly. Analyses of old SLAC data [32] and of more recent data from the European Muon Collaboration (EMC) [33] suggest [31]

$$\Delta u=0.77\ ,\quad \Delta d=-0.49\ ,\quad \Delta s=-0.15 \tag{38}$$

for the polarized quark densities in the proton; in case of the neutron, the u and d quark densities have to be interchanged as usual. The errors of the quantities (38) are about ± 0.08. Very recently, data on polarized lepton-neutron scattering have become available [34]. A recent analysis [35] of these data gives values for the Δq very close to those in Eq. (38), but with somewhat reduced errors.

We are now in a position to present numerical results for LSP-nucleon scattering. We begin with a discussion of the squark exchange contributions to the spin-independent interaction via the f_q term in Eq. (11) as well as via the B_D terms in Eq. (17). As mentioned in the Introduction, this was the first spin-independent contribution to be studied quantitatively [12,13] using effective Lagrangian techniques. We write the scalar contribution to the effective LSP-nucleon interaction as

$$\mathcal{L}_{\rm scalar}^{\chi N}=f\bar{\chi}\chi\bar{\Psi}_N\Psi_N\ , \tag{39}$$

where Ψ_N denotes the nucleon N. In the treatment of Refs. [12,13], the squark exchange contribution to the coefficient f is

$$f_D^{\rm eff}=m_N\left[\sum_{u,d,s}\frac{f_q^{(\tilde{q})}}{m_q}f_{Tq}+\frac{2}{27}f_{TG}\sum_{c,b,t}\frac{f_q^{(\tilde{q})}}{m_q}\right]\ , \tag{40}$$

where $f_{TG}=1-\sum_{u,d,s}f_{Tq}$. The coefficients $f_q^{(\tilde{q})}$ are the squark exchange contributions[8] to Eq. (11a), and the subscript D indicates that we are only including terms proportional to the difference of couplings $a_{\tilde{q}}^2-b_{\tilde{q}}^2$ here. In contrast, we treat the contribution from heavy quarks in exact one-loop approximation as described in Sec. III:

$$f_D=m_N\left[\sum_{u,d,s}\frac{f_q^{(\tilde{q})}}{m_q}f_{Tq}-\frac{8\pi}{9\alpha_S}f_{TG}\left[B_D-\frac{m_\chi^2}{4}B_{1D}\right]\right]\ . \tag{41}$$

Predictions from Eqs. (40) and (41) are compared in Fig. 2. Here and in the following figures, we have chosen a common soft breaking mass $m_{\tilde{q}}$ for all squarks, but we include squark mass splitting due to "D terms" as well as L-R squark mixing [see Eqs. (4)]. We also assume the usual unification relation [2] $M_1=\frac{5}{3}\tan^2\theta_W M_2$ between the SUSY-breaking U(1) and SU(2) gaugino masses. Finally, in this "global SUSY" scenario we assume that $m_{\tilde{q}}$, M_2, the Higgs boson (Higgsino) mass parameter μ, the ratio of vacuum expectation values (VEV'S) $\tan\beta$, the trilinear soft breaking parameter A (which we also assume to be the same for all squarks), the pseudoscalar Higgs boson mass m_P, and the top mass m_t can all be varied independently. In Fig. 2 we have chosen $m_{\tilde{q}}=M_2=200$ GeV, $m_P=500$ GeV, $m_t=140$ GeV, $A=0$, and $\tan\beta=10$.

The solid curves show the predictions of our "exact"

[8] Recall that f_q/m_q is finite as $m_q\to 0$.

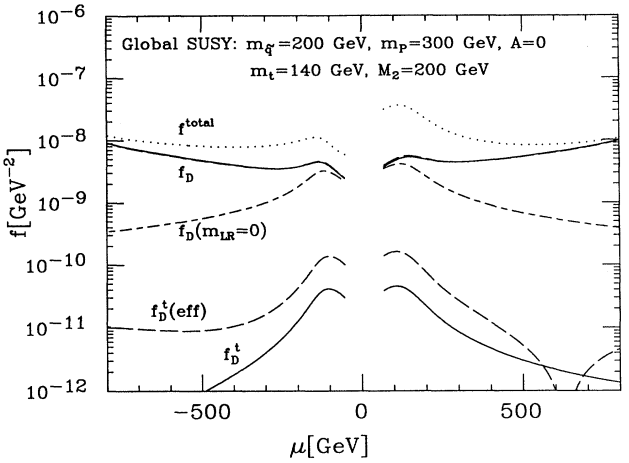

FIG. 2. Squark exchange contributions $\propto a_{\tilde{q}_i}^2 - b_{\tilde{q}_i}^2$ to the spin-independent effective coupling f of Eq. (39). The solid and long-dashed lines show results from our "exact" treatment (41) and the traditional approach (40), respectively; the upper (lower) set of curves is for the total (top-quark–top-squark) contribution. The long-short-dashed lines show the prediction from Eq. (40) if squark mixing is neglected. The dotted curves depict the total result for f, including terms $\propto a_{\tilde{q}_i}^2 + b_{\tilde{q}_i}^2$ and Higgs boson exchange contributions. The curves are not extended into the experimentally excluded region of $|\mu|$.

treatment (41); the upper curves show the total contribution, while the lower curves show the top (s)quark contribution alone. The long-dashed curves have been obtained from Eq. (40) including squark mixing in the approximate treatment of Ref. [13], while the long-short-dashed curves correspond to the treatment of Ref. [12] where squark mixing was ignored. Finally, the dotted curves show the total spin-independent contribution, as discussed in more detail below.

We observe that the effect of squark mixing is quite important everywhere, except at small values of $|\mu|$ where χ is Higgsino-like and the expected relic density Ωh^2 very small. The importance of squark mixing grows with $|\mu|$ since the off-diagonal entries of the squark mass matrices (4) are $\propto \mu$. On the other hand, the approximate treatment of Ref. [13] can be brought into good agreement with our "exact" result for the total f_D. To achieve such a good agreement, we have modified the squark propagators in f_q [Eq. (11a)] slightly, setting $m_q = 0$ for all quarks; moreover, in order to avoid a spurious pole in the top contribution, we have replaced the stop propagators simply by $1/m_{\tilde{t}}^2$. This treatment is rather *ad hoc*, of course, but neither omitting m_χ^2 in all squark propagators (as in the original treatment of Ref. [13]) nor including it everywhere gives nearly as good an approximation to the full result. The lower curves show that this treatment still overestimates the top (top squark) contribution significantly, since the loop integral I_1 is strongly suppressed for $m_q > m_\chi$; this effect cannot be treated properly in the framework of Refs. [12] and [13]. Nevertheless, it affects the total f_D only in the comparatively uninteresting case of a Higgsino-like LSP.

Finally, Fig. 2 shows that the inclusion of squark mixing reduces the dependence of f_D on μ. From Eqs. (8), (9), and (11a), we see that $f_q^{(\tilde{q})}$ gets contributions from Higgsino-gaugino mixing ($\propto X_{q0}Z_{q0}, Y_{q0}Z_{q0}$), as well as from squark mixing ($\propto \sin 2\theta_q X_{q0}Y_{q0}$). The former contribution decreases with increasing $|\mu|$, while the latter increases. Altogether, one can write schematically, for a b-ino-like LSP and small squark mixing angle θ_q,

$$f_q^{(\tilde{q})} \sim \frac{g^2 \tan\theta_W}{2(m_{\tilde{q}}^2 - m_\chi^2)} \left[c_1 \frac{y_L + y_R}{2} \frac{m_q}{\mu + M_2} + c_2 \frac{m_{LR}^2}{m_{LL}^2 + m_{RR}^2} y_L y_R \tan\theta_W \right], \tag{42}$$

where m_{LL}^2, etc., are again elements of the squark mass matrices (4), $y_{L,R}$ are hypercharges, and c_1 and c_2 are numbers of order 1.

In Fig. 3 we show various Higgs boson exchange contributions to the parameter f of Eq. (39):

$$f_H = \left[\sum_{u,d,s} \frac{f_q^{(H)}}{m_q} f_{Tq} + \frac{2}{27} f_{TG} \sum_{c,b,t} \frac{f_q^{(H)}}{m_q} \right] m_N + \frac{8\pi}{9\alpha_S} f_{TG} m_N T_{\tilde{q}} \, . \tag{43}$$

Here $f_q^{(H)}$ is the Higgs boson exchange contribution to the coefficient f_q of Eq. (11a) and $T_{\tilde{q}}$ appears in the effective Lagrangian (17). In Fig. 3 we have fixed $m_{\tilde{q}} = -\mu = 300$ GeV, $m_P = 500$ GeV, $m_t = 140$ GeV, and

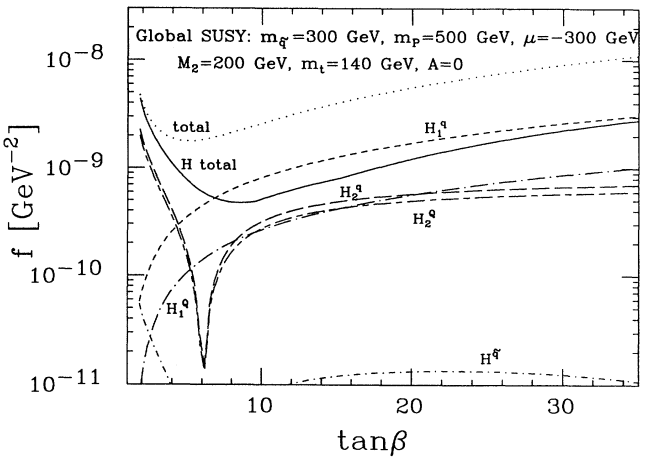

FIG. 3. Higgs boson exchange contributions to the effective coupling f of Eq. (39) [see Eq. (43)]. The solid curve shows the total Higgs boson exchange contribution, the long-dashed and long–short-dashed curves show the light Higgs boson exchange contributions involving light (u,d,s) and heavy (c,b,t) quarks, respectively, and the short-dashed and dot–long-dashed curves depict the corresponding heavy Higgs boson exchange contributions. The dot–short-dashed curve shows the contribution from the last term in Eq. (43), while the dotted curve again depicts the total result for f.

$A=0$ and varied $\tan\beta$. The leading radiative corrections from the top-quark–top-squark sector to the masses and mixing angle of the scalar Higgs bosons [36] have been taken into account.

For the given choice of parameters, squarks are quite heavy, and hence the contribution from squark loops (dot–short-dashed line) is very small; we found previously [16] that it can become sizable only for nonvanishing A. In Fig. 3 the heavy scalar Higgs boson H_1 is approximately degenerate with the pseudoscalar and hence is even heavier than the squarks. Nevertheless, H_1 exchange dominates the total Higgs boson contribution for $\tan\beta \geq 5$. There are two reasons for this: First, the $H_2\chi\chi$ coupling (A2b) goes through zero at $\tan\beta \simeq 6$ as a result of a cancellation between two terms. Second, in the relevant limit $m_P^2 \gg m_Z^2$, the coupling of H_2 to quarks are almost identical to that of the SM Higgs boson, independent of $\tan\beta$. On the other hand, the couplings of H_1 to down-type quarks are enhanced at large $\tan\beta$. Finally, we note that for our choice (36) for the strange quark matrix element f_{Ts} the light quark contribution is actually larger than the one from heavy quark loops. This is especially true for H_1 exchange, since here effectively only down-type quarks contribute once $\tan\beta > 3$ or so. We have to keep in mind, however, that the contribution from light quarks is uncertain to a factor of 2 or so, while the heavy quark contribution depends only weakly on f_{Ts}.

As already emphasized in the Introduction, Higgs bosons can only couple to the LSP if it has both Higgsino and gaugino components. These couplings will therefore be suppressed for large $|\mu|$ and/or $|M_2|$, since in this limit the LSP becomes an almost pure state [7,22]. The overall order of magnitude of the Higgs boson exchange contribution for a b-ino-like LSP can be estimated as

$$f_q^{(H)} \simeq \frac{g^2 \tan^2\theta_W}{4} \frac{m_q}{M_2+\mu} \left[\frac{c_3}{m_{H_2}^2} + \frac{c_4 (\tan\beta)^{-2I_{3q}}}{m_{H_1}^2} \right], \tag{44}$$

where c_3 and c_4 are again numerical factors of order 1 and the exponent in the second term describes the enhancement (suppression) of the H_1 coupling to up (down) quarks.

In Fig. 4 we show contributions to the χN interaction parameter f of Eq. (39) that are proportional to the sum of couplings $a_{\tilde{q}_i}^2 + b_{\tilde{q}_i}^2$; none of these contributions have been taken into account in the existing literature. In order to write these contributions in the form of Eq. (39), we use Eqs. (22) and (33) as well as the identities

$$\bar{\chi}\gamma_\mu \partial_\nu \chi = -\frac{i}{m_\chi} k_\mu k_\nu \bar{\chi}\chi , \tag{45a}$$

$$(p_\mu p_\nu - \tfrac{1}{4} m_N^2 g_{\mu\mu}) k_\mu k_\nu = \tfrac{3}{4} m_N^2 m_\chi^2 , \tag{45b}$$

where p and k are the momenta of the nucleus N and LSP χ, respectively, and we have omitted terms proportional to the LSP velocity v. The total result is

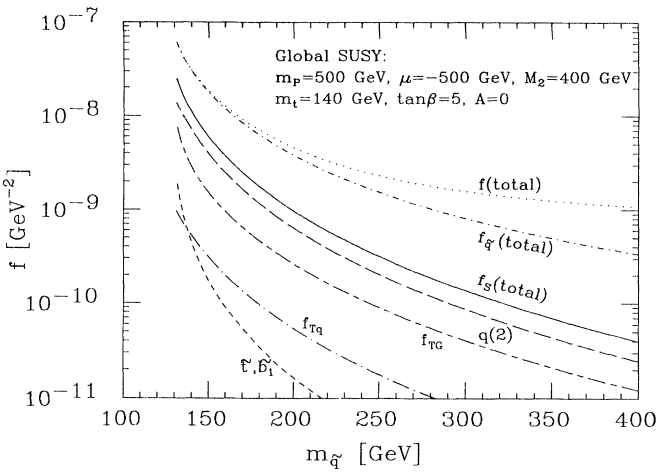

FIG. 4. Squark exchange contributions $\propto a_{\tilde{q}_i}^2 + b_{\tilde{q}_i}^2$ to the effective coupling f of Eq. (39) [see Eq. (46)]. The solid line shows the total f_S, while the dot–long-dashed, long–short-dashed, and long-dashed curves show the contributions from the first, second, and fourth terms in Eq. (46). The short-dashed curve shows the contribution from the third term in Eq. (46), where we have also included $\tilde{b}_1$ exchange as described in the text. The dot–short-dashed and dotted curves show the total squark exchange contribution to f and the total result for f, including Higgs boson exchange, respectively.

$$\begin{aligned} F_S = {} & \tfrac{1}{2} m_\chi m_N \sum_{u,d,s} g_q f_{Tq} \\ & + \frac{8\pi}{9\alpha_S} \left[B_S - \frac{m_\chi}{2} B_{2S} - \frac{m_\chi^2}{4} B_{1S} \right] f_{TG} m_N \\ & + \frac{3}{2} \left[B_{2S}^t + \frac{m_\chi}{2} (B_{1S}^t + B_{1D}^t) \right] m_N m_\chi G(m_t^2) \\ & - \tfrac{3}{2} \sum_{u,d,s,c,b} g_q q(\mu_0^2) m_N m_\chi . \end{aligned} \tag{46}$$

The first term comes from the trace over the twist-2 quark operators [see Eq. (13)]. The second term originates from the trace of the twist-2 gluon operator, as discussed in Sec. III A. The third term is the top-quark (top-squark) contribution to the gluonic twist-2 operator; as discussed in Sec. III B, we always treat this contribution in an exact one-loop approximation. The last term in Eq. (46) gives the light quark contribution to twist-2 operators, evaluated according to Eq. (32). Recall that for small mass difference $m_{\tilde{b}_1} - m_\chi$ the contribution from the lighter bottom squark eigenstate is also treated in exact one-loop order, as discussed in detail at the end of Sec. III B. In Fig. 4 we therefore show the $\tilde{b}_1$ contribution together with $\tilde{t}$ contribution. We see from Fig. 4 that the last term in Eq. (46) dominates, followed by the second term. The other two contributions are usually negligible. The overall order of magnitude of f_S for a b-ino-like LSP is

$$f_S \sim \frac{g^2 \tan^2\theta_W}{4} \sum_q \frac{y_q^2}{(m_{\tilde{q}}^2 - m_\chi^2)^2} q(2) m_\chi m_N . \tag{47}$$

Comparison with Eq. (42) shows that f_S falls off faster with increasing squark mass than the contribution $\propto a_{\tilde{q}_i}^2 - b_{\tilde{q}_i}^2$. This is also demonstrated by the dot-short-dashed curve in Fig. 4, which shows the total contribution from squark exchange. At small $m_{\tilde{q}}$ the contributions are compatible; moreover, since here $f_q^{(\tilde{q})}$ is dominated by the second term in Eq. (42), the curves also have similar slopes. However, for heavier squarks the first term dominates Eq. (42), and the total squark exchange contribution drops less rapidly with increasing $m_{\tilde{q}}$ than f_S does.

B. Counting rate in a germanium detector

Having discussed the relative importance of various contributions to the spin-independent LSP-nucleon scattering amplitude, we are now in a position to present numerical results for elastic LSP scattering off heavy target nuclei. We choose germanium isotopes for this discussion, since a new class of germanium detectors with increased sensitivity for DM searches is expected to become operational in the near future [37]. The relevant quantity for direct search experiments is the interaction rate which is usually measured in events/(kg day). It is given by

$$R = \frac{\sigma\xi}{m_\chi m_A} \frac{1.8\times10^{11}\ \text{GeV}^4}{(\text{kg day})} \frac{\rho_\chi}{0.3\ (\text{GeV/cm}^3)} \times \frac{\bar{u}_\chi}{320\ (\text{km/sec})} . \tag{48}$$

Here m_A is the mass of the nucleus under consideration, ρ_χ is the *local* LSP mass density, and $\bar{u}_\chi$ the average or effective LSP density that results from integrating over the (assumed) Maxwellian velocity distribution of the LSP [38]. The elastic LSP-nucleon cross section for the idealized case of a pointlike nucleon is given by

$$\sigma = \frac{4m_\chi^2 m_A^2}{\pi(m_\chi+m_A)^2} \left\{ [Zf_p + (A-Z)f_n]^2 + 4\lambda^2 J(J+1) \left[\sum_{u,d,s} d_q \Delta q \right]^2 \right\} . \tag{49}$$

Here Z and A are the charge and isotope number of the nucleus; recall that the contribution $\propto f_{Tu}, f_{Td}$ as well as the u- and d-quark densities are different for protons and neutrons. J is the total spin of the nucleus, and λ is a nucleonic matrix element that basically describes the fraction of the total spin that is due to the spin (rather than the orbital angular momentum) of the nucleons. As usual in the literature [10–12,18,19], we will assume that only a single "valence" nucleon contributes to the total spin, so that the sum in the second term of Eq. (49) runs over the polarized parton densities of either a proton or a neutron. We refer the interested reader to Ref. [39] for a more comprehensive treatment of the nuclear physics of LSP-nucleus scattering. For our case of ^{73}Ge, we adopt the value [18] $\lambda^2 J(J+1) = 0.065$.

Finally, the factor ξ in Eq. (48) describes the suppression due to nuclear form factors. Ellis and Flores [18] found that Gaussian form factors describe the total counting rate adequately. For the standard assumptions about the LSP velocity distributions, one has [18]

$$\xi = \frac{0.573}{B} \left\{ 1 - \frac{\exp[-B/(1+B)]}{\sqrt{1+B}} \frac{\text{erf}[\sqrt{1/(1+B)}]}{\text{erf}(1)} \right\} , \tag{50}$$

where erf is the error function and

$$B \equiv \frac{m_\chi^2 m_A^2}{(m_\chi+m_A)^2} \frac{8}{9} r^2 \bar{v}_\chi^2 , \tag{51}$$

with $\bar{v}_\chi \simeq \bar{u}_\chi/1.2$ being the "velocity dispersion" [38]. For the spin-independent interaction, we use $r = r_{\text{charge}} = (0.3 + 0.89 A^{1/3})$ fm, while for the spin-dependent interaction of ^{73}Ge we use a slightly softer form factor[9] [18] with $r_{\text{spin}} = 1.25 r_{\text{charge}}$.

In Figs. 5(a)–5(c) we show contours of constant counting rate in the plane $(M_2, m_{\tilde{q}})$, where M_2 is the SU(2) gaugino mass and $m_{\tilde{q}}$ the SUSY-breaking contribution to squark masses, which we assume to be identical for all squarks. We have fixed $\mu = m_P = 300$ GeV and take a top mass of 140 GeV. In Figs. 5(a) and 5(b) we have chosen $\tan\beta = 2$, while Fig. 5(c) is for $\tan\beta = 8$. In all figures the central region between the dotted lines is excluded by constraints from unsuccessful sparticle searches at the CERN e^+e^- collider LEP [40], and the regions below the dotted lines at large $|M_2|$ and small $m_{\tilde{q}}$ are excluded by the requirement $m_\chi \le m_{\tilde{\tau}_1}$. Finally, in the hatched regions relic LSP's would overclose the universe ($\Omega h^2 > 1$), while in the shaded region the LSP relic abundance is too small to account for a significant fraction of the observed dark matter ($\Omega h^2 < 0.05$).

In Figs. 5(a) and 5(b) we observe large differences between the regions of positive and negative M_2. (More precisely, only the sign of the product $\mu M_2 \tan\beta$ is relevant here.) For given $|M_2|$, the LSP is slightly lighter and has a considerably larger Higgsino component if $M_2 > 0$. This enhances the couplings to Higgs and Z bosons, and increases the first contribution to $f_q^{(\tilde{q})}$ in Eq. (42), which is due to neutralino mixing. Furthermore, there is a cancellation in the $H_2\chi\chi$ coupling for $M_2 < 0$ [22]. As a result, the expected counting rate is generally larger and the LSP relic density smaller for positive M_2. Unfortunately, this correlation implies that often combinations of parameters that lead to a large counting rate for fixed local LSP density also lead to such a low universal relic abundance that the LSP does not make a good DM candidate any more. This is demonstrated by the re-

[9] Our expression of counting rate (48) and (49) is 4 times larger than the result given in Ref. [18]. As stated earlier, the scattering amplitudes that one derives from the effective Lagrangians (1) and (39) have to include a factor of 2 due to the Majorana nature of the LSP. Our spin-dependent cross section (49) agrees with Ref. [12].

gion of large positive M_2 in Figs. 5(a) and 5(b), where almost the entire region with counting rate >0.1 event/kg day) also has relic density $\Omega h^2<0.05$. This correlation has previously been observed in Ref. [41], where only the light Higgs boson exchange contribution was taken into account. On the other hand, for the given choice of parameters there are large regions in the (M_2,μ) plane where LSP does make an interesting DM candidate and the counting rate is larger than 0.02 event/(kg day), if $M_2>0$; for $M_2<0$, the counting rate is at most a few times 10^{-3} events/(kg day) unless $m_{\tilde{q}}$ is close to m_χ.

Comparison of Figs. 5(a) (for ^{76}Ge) and 5(b) (for ^{73}Ge) shows that the spin-dependent contribution to the cross section is quite small. In most cases the ^{73}Ge counting rate is even slightly smaller than the ^{76}Ge rate as a result of the smaller coherence enhancement factor. The only exception occurs in the region of small $m_{\tilde{q}}$ and small negative M_2, where the LSP is photinolike and the spin-dependent squark exchange contribution is sizable. In this particular case the ^{73}Ge counting rate can be as much as 50% larger than the ^{76}Ge rate. However, usually the difference in counting rate is of order 10% or less. A pure-isotope detector does therefore not seem to offer much of an advantage over a detector using the natural mix of Ge isotopes.

At $\tan\beta=8$ [Fig. 5(c)], the region with large counting rates has shrunk considerably. Even in the half-plane of positive M_2 the counting rate now often falls below 0.02 events/(kg day). One reason is that increasing $\tan\beta$ from 2 to 8 increases the mass of the light Higgs boson by approximately 50%. In addition, b-ino–Higgsino mixing is suppressed (enhanced) compared to the case $\tan\beta=2$ for positive (negative) M_2. Both effects conspire to reduce the counting rate and increase the relic density for $M_2>0$. In addition, for $M_2<0$ the contributions from the exchange of the heavy and light Higgs scalars often

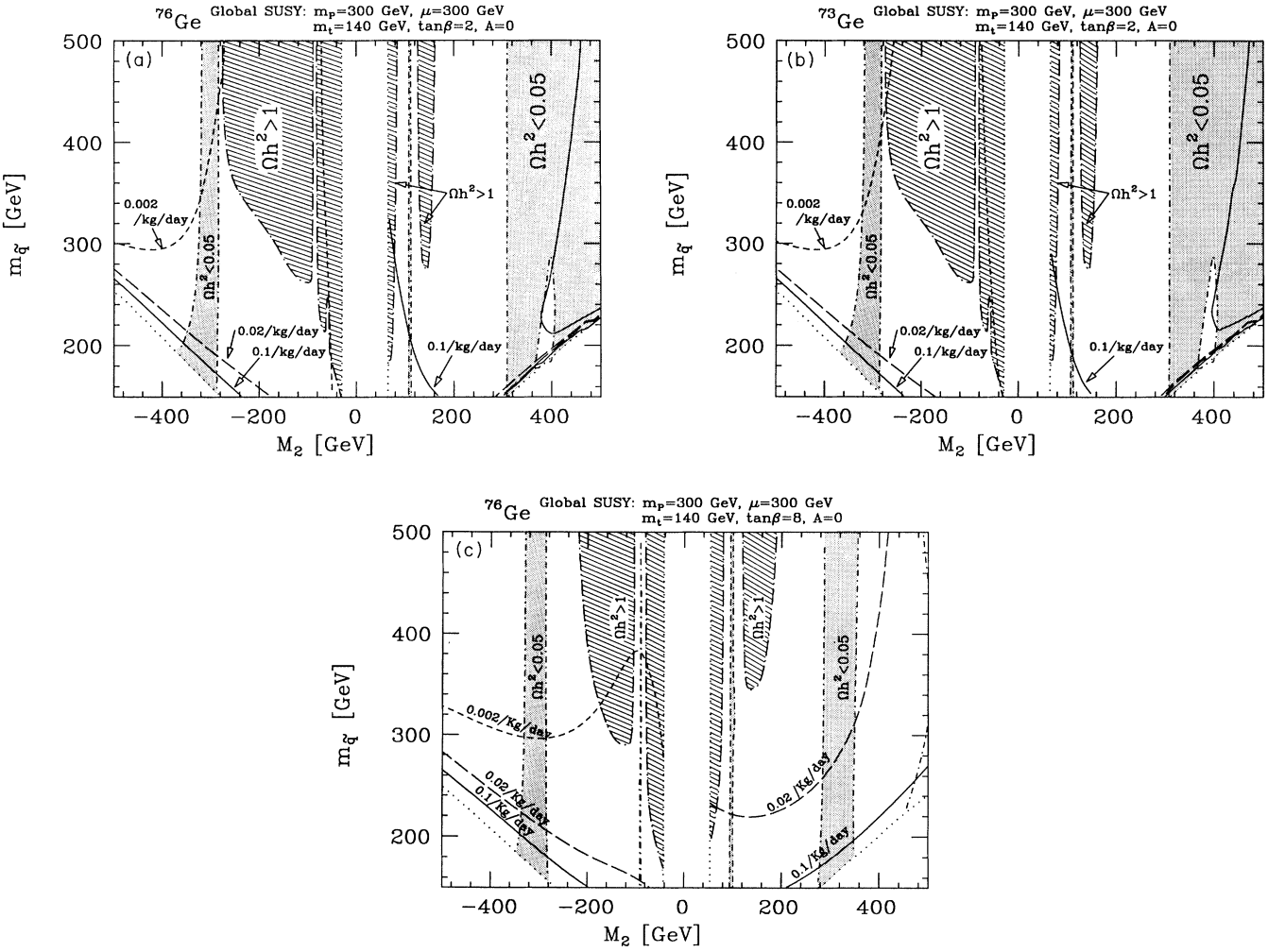

FIG. 5. Contours of constant counting rate [in events/kg day)] in a germanium detector. The region between the dotted lines at small $|M_2|$ is excluded by sparticle searches, while the regions below the dotted curves at small $m_{\tilde{q}}$ and large $|M_2|$ are excluded because here the LSP is charged. In the hatched regions labeled $\Omega h^2>1$, relic neutralinos overclose the Universe, while in the shaded regions the relic density is too small to make the LSP an interesting DM candidate. (a) and (c) are for a pure ^{76}Ge detector with $\tan\beta=2$ and 8, respectively, while (b) is for a pure ^{73} Ge detector and $\tan\beta=2$.

tend to cancel (see Fig. 3); this explains why the region with very small counting rate, below 2×10^{-3}, is much larger in Fig. 5(c) than in Fig. 5(a). On the other hand, large tanβ also enhances $\tilde{b}$ and $\tilde{s}$ squark mixing and reduced $\tilde{c}$ squark mixing [see Eqs. (4)]. Since the $\tilde{b}$ and $\tilde{c}$ contributions tend to cancel for $M_2<0$, this results in an increase of f_D in Eq. (41), by more than a factor of 5. This explains the growth of the region with counting rate ≥ 0.02 events/(kg day) in the half-plane with negative M_2. Finally, we remark that at large $|\tan\beta|$ the sign of $M_2\mu\tan\beta$ is less important than for small $|\tan\beta|$; in the limit $|\tan\beta|\to\infty$, this sign becomes irrelevant.

So far, we have only considered "global SUSY" models where $m_{\tilde{q}}$, m_P, M_2, μ, tanβ, A, and m_t can all be varied independently. From the theoretical point of view, "minimal" supergravity (SUGRA) models [2] are more attractive. These models do not only allow one to describe potentially realistic sparticle spectra with fewer parameters, they can also explain (rather than parametrize) electroweak gauge symmetry breaking in terms of radiative corrections to the Higgs potential. In these models supersymmetry breaking is described by a common scalar mass m_0, a common gaugino mass $m_{1/2}$, and a common A parameter. This degeneracy is assumed to be exact only at some very-high-energy scale, e.g., the unification scale M_X. At lower scales the masses of different scalars and different gauginos differ due to quantum corrections, which can be described by a set of coupled renormalization group equations (RGE's) [42]. In the remaining two figures, we have used simple analytical parametrizations [21,22] of the exact numerical solutions of these equations. Moreover, we have required the correct amount of gauge symmetry breaking, i.e., the correct W mass at the weak scale. This leaves us with altogether five free parameters,[10] which we take to be the SU(2) gaugino mass M_2 at the weak scale, m_t, A, m_0, and tanβ. Note that μ and m_P are derived quantities in this scheme.

In Fig. 6 we show contours of constant counting rate in a ^{76}Ge detector in the (M_2,m_0) plane for $m_t=140$ GeV, $A=0$, and tan$\beta=2$. We immediately see that the counting rate is much smaller than in Fig. 5. One reason is that now squarks of the first two generations are at least 5 times heavier than the LSP. This is because the RGE's lead to a positive contribution $\simeq 8M_2^2$ to squared on-shell squark masses, while we still have $|m_\chi|\leq|M_1|\simeq|M_2|/2$. As a result, the total squark exchange contribution is usually just a few % or even less of the Higgs boson exchange contribution. Therefore Fig. 6 shows no regions of large counting rate for large $|M_2|$ and small m_0, although some combinations of parameters are still excluded by demanding the LSP to be electrically neutral; the light charged sparticle in this case is the light $\tilde{\tau}$ state, however, which is much lighter than the lightest squark [21].

Another reason for the small counting rate is that we now always have $\mu\geq|M_2|$, since μ is fixed by the condition to get correct symmetry breaking. Therefore χ is always an almost pure gaugino state in this figure, usually a b-ino. The lines of constant counting rate almost coincide with lines of constant M_2; large $|M_2|$ implies larger μ and smaller $\chi\chi H$ couplings [see Eq. (44)]. For the given choice of m_t, A, and tanβ, μ increases very slowly with m_0. Larger values of m_0 also imply larger values of the light Higgs boson mass, because of increasing top-quark–top-squark loop corrections [36]. These two effects explain the m_0 dependence of the counting rate. Finally, the mass of the pseudoscalar Higgs boson also increases with $|M_2|$ and m_0. As a result, m_P is always well above $2m_\chi$, and there is no region of small relic density at large $|M_2|$. Instead, we find an unacceptably large relic density at large m_0 and $|M_2|\geq 100$ GeV, because the dominant slepton exchange diagrams are suppressed here; see Ref. [22] for a discussion of the LSP relic density in minimal SUGRA.

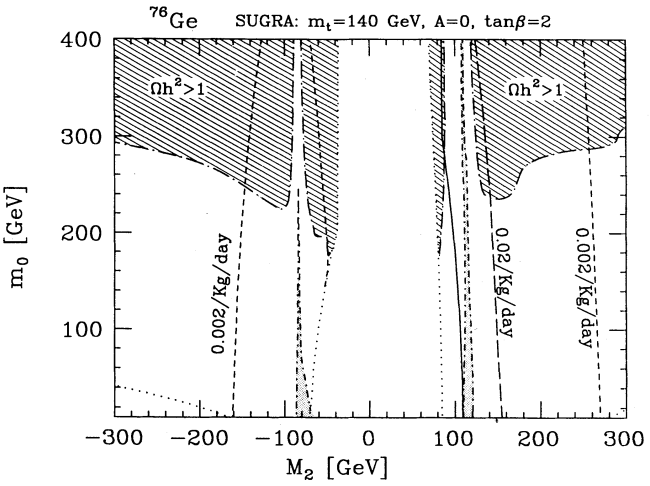

FIG. 6. Contours of constant counting rate in a ^{76}Ge detector as predicted in a minimal supergravity model with radiative symmetry breaking. The notation is as in Fig. 5.

The results of Fig. 6 do not depend strongly on m_t and A. Larger m_t implies larger μ and less neutralino mixing as well as larger Higgs boson masses, leading to smaller counting rates, but for $M_2<0$ the rate only changes by a factor of 2 or so when m_t is increased to 170 GeV or reduced to 110 GeV. For $M_2>0$ the dependence on m_t is stronger, since the Higgsino component of χ is not only larger here, it also increases faster with decreasing μ. Similar remarks also apply for the A dependence. If $AM_2>0$, both μ and m_{H_2} increase with $|A|$, and the counting rate decreases. However, very large values of $|A|$ are excluded because the lighter $\tilde{t}$ squark would become too light.

On the other hand, the counting rate does depend quite strongly on tanβ, as illustrated in Fig. 7. Since the cross section is always dominated by Higgs boson exchange contributions, the overall shape of the curves resembles the square of the solid curve in Fig. 3. However, there are some important differences. In the region of small tanβ, μ increases rapidly with tanβ [21], which reduces

[10]Unlike in Ref. [21], we do not assume $B(M_X)=A-m_0$ here.

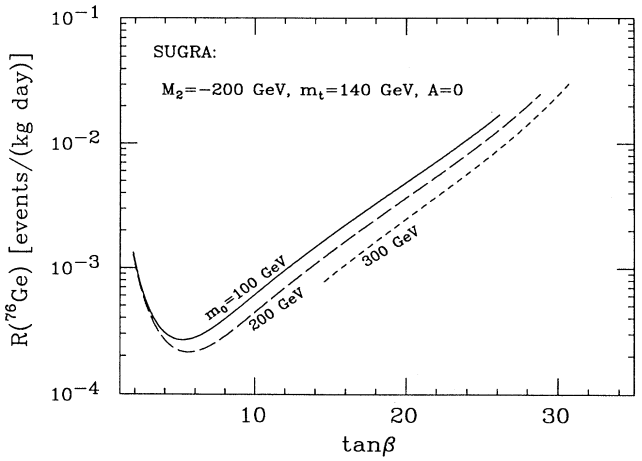

FIG. 7. tanβ dependence of the counting rate as predicted in minimal supergravity. Different curves correspond to different values of the common scalar mass m_0 at scale M_X, as indicated. The curves are terminated at high tanβ where the rescaled relic density Ωh^2 falls below 0.05. For $m_0=300$ GeV one has $\Omega h^2>1$ for tan$\beta\leq 14$.

the $H\chi\chi$ couplings. This partly compensates the reduction of m_{H_2} at small tanβ. Once tan$\beta\geq 5$ or so, μ becomes almost independent of tanβ. However, m_P and hence the mass of the heavier Higgs boson H_1 decrease at large values of tanβ; recall that H_1 exchange is much more important than H_2 exchange[11] once tan$\beta>15$. Near the end of the curves, squark exchange contributes about 10–15 % of the total scattering amplitude as a result of enhanced Yukawa couplings and enhanced squark mixing in the s,b squark sectors. Together with the reduction of m_{H_1}, this implies a faster increase of the counting rate than what one would expect from Fig. 3, where m_P was taken constant. Eventually, m_P is reduced to a value close to $2m_\chi$, and the LSP relic density drops below 0.05 [22]; we have terminated the curves at this point. Finally, we see that for large tanβ the counting rate does depend on m_0. This is because m_{H_1} increases with m_0. However, this dependence is clearly still much weaker than the dependence on tanβ.

V. SUMMARY AND CONCLUSIONS

In this paper we presented a detailed discussion of elastic LSP-nucleon scattering with emphasis on the role played by strong interactions. We have little to add to the present understanding of the spin-dependent contribution to the scattering amplitude, because the operators $\bar{q}\gamma_\mu\gamma_5 q$ that appear in the spin-dependent effect LSP-quark interaction of Eq. (1) are not renormalized by strong interactions if $m_q=0$. In other words, the quantities Δq that one introduces to parametrize the hadronic matrix elements of these operators do not depend on the renormalization scale.

On the other hand, QCD effects are crucial for the understanding of spin-independent LSP-nucleon interactions. Such interactions would be absent in a world where chirality is conserved exactly. In the case at hand, chirality breaking can enter either via the quark mass or via the LSP mass. In previous studies [12–15,18] only terms $\propto m_q$ were included. Both Higgs boson and squark exchanges contribute to these terms; the hadronic matrix elements $\langle N|m_Q\bar{Q}Q|N\rangle$ that relate LSP-quark scattering to LSP-nucleon scattering were treated using the result of Ref. [15]. We argued in Sec. III A that this is strictly speaking not correct for the squark exchange contribution, since it involves the evaluation of a loop integral with one propagator contracted to a point. We were nevertheless able to find a modification of this "effective" treatment of Refs. [12,13] that usually reproduces the full one-loop calculation [16] for the total heavy quark contribution quite accurately. However, this treatment fails for the top quark contribution. For the cases we checked, this changed the total squark exchange contribution by more than ~20% only if the total amplitude was dominated by the Higgs boson exchange terms. However, in models where the top (s)quark contribution is enhanced, this "effective" treatment may no longer be sufficient. Finally, we emphasize that mixing between the superpartners of left- and right-handed quarks is usually important [13] whenever the squark exchange contribution is sizable. Squark mixing is as generic a prediction of SUSY models as LSP mixing is; ignoring it can therefore give quite misleading results.

The existence of terms where chirality is broken by the LSP mass rather than the quark mass has previously been noted by us [16]. In Secs. II and III B of this paper, we discussed the connection between these terms and the "twist-2" operators that appear in analyses of deep inelastic lepton-nucleon scattering. We used the QCD-improved parton model which automatically resums leading logarithmic corrections to all orders in perturbation theory. This is quite important, reducing the contribution from b and c (s)quarks to these terms by a factor of 2 or more, compared to the one-loop result. We emphasize again that this class of contributions survives even in the limit of no squark mixing and no mixing in the neutralino sector, unlike the other coherent contributions. On the other hand, this new contribution is proportional to $m_{\tilde{q}}^{-4}$, while the previously discussed squark exchange contribution is $m_{\tilde{q}}^{-2}$. Within the MSSM this contribution is therefore only numerically important if squarks are not much heavier than the LSP.

It should be kept in mind that all squark exchange contributions are usually subdominant if squarks are very heavy. If we simply multiply all mass parameters in the neutralino and squark sectors of the theory with a constant factor (keeping m_W fixed), all coherent squark exchange contributions scale with the inverse third power of this factor; this can most easily be seen from our approximate expressions (42) and (47) given in Sec. IV A. We also find that the spin-dependent amplitude decreases

[11]This also implies that the total counting rate in this region of parameter space strongly depends on the value f_{Ts} of the hadronic matrix element $\langle N|m_s\bar{s}s|N\rangle$, which is uncertain to a factor of 2 or so.

as the inverse second power of this overall mass scale. The Higgs sector behaves differently, because it has to give the correct symmetry breaking. The heavy Higgs boson exchange contribution again falls with the third power of this scale. However, the light Higgs boson exchange contribution (44) only decreases linearly as a result of reduced neutralino mixing. This comes from the well-known fact [36] that the mass of the light Higgs boson is bounded from above in the MSSM, almost independently of the overall sparticle mass scale. Similar bounds can be derived even if nonminimal models [43]. We thus find that for sufficiently heavy sparticles, light Higgs boson exchange will always dominate the total LSP-nucleus scattering cross section. Of course, increasing all sparticle masses arbitrarily not only leads to fine-tuning problems; it can also easily lead to an unacceptably large cosmological relic density [7].

In Sec. IV B we used our LSP-nucleon scattering amplitude to compute relic neutralino scattering rates in a germanium detector. We found that these rates depend quite strongly on the parameters of the model, as indicated by the above scaling law. Even the relative sign of parameters of the neutralino mass matrix was found to be very important. The proposed detectors [37] aim for a sensitivity of about 0.1 event/(kg day). We see from Fig. 5 that such a large counting rate can usually only be expected if either the light Higgs boson or the LSP itself is quite light; both cases should be testable at the second phase of the LEP collider. In order to arrive at this conclusion, we exclude combinations of parameters that lead to a very small overall LSP relic density, since in such a situation the LSP is obviously not a good DM candidate. We also find that usually, although not always, the spin-dependent interaction is too small to be detectable.

The situation simplifies somewhat in the more restrictive minimal supergravity models. Unfortunately, here the expected counting rate is usually quite low. Indeed, we often are in the "asymptotic" region discussed above, where only the light Higgs boson exchange contribution survives, unless the ratio of vacuum expectation value $\tan\beta$ is large, in which case the exchange of the behavior Higgs boson makes the dominant contribution. The least favorable situation occurs at intermediate values of $\tan\beta$ where the counting rate could fall well below 10^{-3} event/(kg day) even for an only moderately heavy sparticle spectrum, as seen in Fig. 7, where $m_\chi \simeq 100$ GeV.

Given that most combinations of parameters give a counting rate well below 0.1 event/(kg day), should we pursue this kind of experiment further? We think the answer to this question is emphatically "yes." First of all, we do not know how nature chose her parameters. There are regions in parameter space not excluded by any experiment that do lead to sizable counting rates. Moreover, as already mentioned in the Introduction, a positive relic LSP signal would yield information that *cannot* be obtained from any collider experiment. For instance, a positive signal would immediately give a lower bound of the order of 10^{10} yr on the LSP lifetime, some 25 orders of magnitude beyond what can be achieved at collider experiments. Moreover, such a signal would obviously greatly enhance our knowledge of how our galaxy has formed.

On the other hand, even if these experiments did reach a sensitivity of 10^{-3} or even 10^{-4} events/(kg day), they would not preempt the motivation for SUSY searches at colliders. This is because the absence of a signal in an LSP search experiment is difficult to translate into stringent bounds on model parameters. We already mentioned that an unstable but long-lived LSP could never be detected in this fashion; this could easily be accommodated by introducing R-parity-breaking interactions at a strength well below possible experimental limits. Furthermore, one has to realize that the expression (48) for the counting rate depends on several parameters beyond those describing the sparticle spectrum. We already mentioned the sizable uncertainty in the strange quark matrix element $\langle N|m_s\bar{s}s|N\rangle$, which can result in as much as a factor of 4 uncertainty in the counting rate. Perhaps even more worrisome is the uncertainty in the local neutralino flux, $\rho_\chi \bar{u}_\chi$ in Eq. (48). Existing studies [44] conclude that this is known to a factor of 2 or so, based on current models of galaxy formation. We are no experts in this field, but to our knowledge no "standard model of galaxy formation" has emerged yet. It should be noted here that the currently accepted best guess value for the local LSP density ρ_χ is some five orders of magnitude larger than the universal relic density. Similar, current estimates of the velocity $\bar{u}_\chi$ are some seven orders of magnitude above the thermal velocity of big bang relics. Together, this gives a "glactic enhancement factor" (compared to the average over the Universe) of $\sim 10^{12}$. Clearly, LSP detection would be hopeless without this enhancement, but can present galaxy formation models really predict this factor up to a factor of 2 or so?

Our conclusion is therefore that sparticle searches at colliders are complementary to LSP detection experiments. Each kind of experiment can yield information not accessible to the other. The results presented in this paper should allow for the as yet most accurate calculation of the cross sections relevant for the analysis of experiments searching for cosmic relic neutralinos.

ACKNOWLEDGMENTS

We thank K. Hikasa, M. Savage, K. Griest, and M. Luke for very useful discussions and suggestions, and X. Tata and D. Zeppenfeld for discussions. M.D. thanks the particle physics group at the University of Hawaii and especially X. Tata for their hospitality during his visit where part of this work was completed. This work was supported in part by the U.S. Department of Energy under Contract No. DE-AC02-76ER00881, and in part by the Wisconsin Research Committee with funds granted by the Wisconsin Alumni Research Foundation. The work of M.D. was supported by a grant from the Deutsche Forschungsgemeinschaft under the Heisenberg program.

APPENDIX A

In this appendix we give explicit expressions for the Z and Higgs boson couplings that enter the effective La-

grangians of Eqs. (1) and (10). We use the notation of Ref. [22], which is very similar to the conventions of Haber and Kane [2] and Gunion and Haber [45]. In particular, we denote the four components of the eigenvector of the 4×4 neutralino mass matrix that corresponds to the LSP (the lightest neutralino) by N_{0i}; $i=1$ corresponds to the b-ino component, $i=2$ the SU(2) gaugino component, and $i=3$ and 4 are the hypercharge $Y=-\frac{1}{2}$ and $+\frac{1}{2}$ Higgsino components, respectively. Note that we take N_{0i} to be real; this means that the sign of the eigenvalue m_χ has to be kept when evaluating the scattering amplitudes. However, the kinematical prefactor in the expression (49) for the cross section only depends on the kinematical mass, i.e., the absolute value of m_χ. Mixing in the Higgs sector is described [45] by the angles β and α; $\tan\beta$ is the ratio of the VEV's of the $Y=+\frac{1}{2}$ and $-\frac{1}{2}$ neutral Higgs bosons, and α describes the mixing of the neutral scalar mass eigenstates.

We are now in a position to list the couplings appearing in the main text. We start with the LSP-Z coupling in Eqs. (2):

$$O''^R=\tfrac{1}{2}(N_{04}^2-N_{03}^2)\ . \tag{A1}$$

Expressions for the LSP-quark-squark couplings have already been given in the main text [Eqs. (8) and (9)].

We next turn to the LSP–Higgs-boson couplings appearing in Eqs. (11a) and (18f). They are given by [45]

$$c_\chi^{(1)}=\tfrac{1}{2}(gN_{02}-g'N_{01})(N_{04}\sin\alpha-N_{03}\cos\alpha)\ , \tag{A2a}$$

$$c_\chi^{(2)}=\tfrac{1}{2}(gN_{02}-g'N_{01})(N_{03}\sin\alpha+N_{04}\cos\alpha)\ , \tag{A2b}$$

where g and g' are the SU(2) and $U(1)_Y$ gauge couplings, respectively. Recall that the superscript 1 refers to the heavier scalar Higgs boson.

The Higgs-boson–quark couplings entering Eq. (11a) can be written as [45] $c_q^{(i)}=gr_q^{(i)}/(2m_W)$, with

$$r_u^{(1)}=-\frac{\sin\alpha}{\sin\beta}\ ,\quad r_d^{(1)}=-\frac{\cos\alpha}{\cos\beta}\ ,$$
$$r_u^{(2)}=-\frac{\cos\alpha}{\sin\beta}\ ,\quad r_d^{(2)}=\frac{\sin\alpha}{\cos\beta}\ ; \tag{A3}$$

here u (d) stands for any charge $=+\frac{2}{3}$ ($-\frac{1}{3}$) quark.

Finally, the diagonal Higgs-boson–squark couplings appearing in Eq. (18f) can be written as (remember that $\tilde q_1=\cos\theta_q\tilde q_L+\sin\theta_q\tilde q_R$ stands for the lighter squark mass eigenstate)

$$c_{\tilde q_1}^{(i)}=\frac{gm_Z}{\cos\theta_W}s^{(i)}(I_{3q}\cos^2\theta_q-e_q\sin^2\theta_W\cos2\theta_q)$$
$$+\frac{gm_q^2}{m_W}r_q^{(i)}-\frac{gm_q\sin2\theta_q}{2m_W}(A_qr_q^{(i)}+\mu r_q'^{(i)})\ , \tag{A4a}$$

$$c_{\tilde q_2}^{(i)}=\frac{gm_Z}{\cos\theta_W}s^{(i)}(I_{3q}\sin^2\theta_q+e_q\sin^2\theta_W\cos2\theta_q)$$
$$+\frac{gm_q^2}{m_W}r_q^{(i)}+\frac{gm_q\sin2\theta_q}{2m_W}(A_qr_q^{(i)}+\mu r_q'^{(i)})\ . \tag{A4b}$$

The parameters A_q and μ enter the off-diagonal elements of the squark mass matrices of Eq. (4), m_W and m_Z are the masses of the weak gauge bosons, θ_W is the weak mixing angle, $I_{3q}=\pm\frac{1}{2}$ and e_q are the third component of the weak isospin and electric charge of quark q, respectively, and the $r_q^{(i)}$ have already been defined in Eq. (A3); finally, $s^{(i)}$ and $r_q'^{(i)}$ are given by

$$s^{(1)}=-\cos(\alpha+\beta)\ ,\quad s^{(2)}=\sin(\alpha+\beta)\ , \tag{A5a}$$

$$r_u'^{(1)}=-\frac{\cos\alpha}{\sin\beta}\ ,\quad r_d'^{(1)}=-\frac{\sin\alpha}{\cos\beta}\ ,$$
$$r_u'^{(2)}=\frac{\sin\alpha}{\sin\beta}\ ,\quad r_d'^{(2)}=-\frac{\cos\alpha}{\cos\beta}\ . \tag{A5b}$$

APPENDIX B: LOOP INTEGRALS

In this appendix we list the loop integrals that appear in Eqs. (18a)–(18e):

$$I_1(m_{\tilde q},m_q,m_\chi)=\int_0^1dx\frac{x^2-2x+\frac{2}{3}}{D^2}$$
$$=\frac{1}{\Delta}\left[\frac{m_q^2-m_\chi^2}{3m_{\tilde q}^2}-\frac{2}{3}\frac{m_{\tilde q}^2-m_\chi^2}{m_q^2}-\frac{5}{3}+\left[2m_{\tilde q}^2-\frac{2}{3}m_\chi^2\right]L\right]\ , \tag{B1a}$$

$$I_2(m_{\tilde q},m_q,m_\chi)=\int_0^1dx\frac{x(x^2-2x+\frac{2}{3})}{D^2}$$
$$=\frac{1}{2m_\chi^4}\left[\ln\frac{m_{\tilde q}^2}{m_q^2}-(m_{\tilde q}^2-m_q^2-m_\chi^2)L\right]$$
$$+\frac{1}{\Delta}\left\{\left[\frac{m_q^4-m_q^2m_{\tilde q}^2}{m_\chi^2}-\frac{7}{3}m_q^2+\frac{2}{3}(m_\chi^2-m_{\tilde q}^2)\right]L+\frac{m_q^2-m_\chi^2}{3m_{\tilde q}^2}+\frac{m_{\tilde q}^2-m_q^2}{m_\chi^2}+\frac{2}{3}\right\}\ , \tag{B1b}$$

$$I_3(m_{\tilde{q}},m_q,m_\chi)=\int_0^1 dx\frac{x^2(1-x)^2}{D^3}$$
$$=\frac{3(m_\chi^2-m_q^2-m_{\tilde{q}}^2)}{\Delta^2}+\frac{L}{\Delta}\left[-1+\frac{6m_q^2m_{\tilde{q}}^2}{\Delta}\right], \tag{B1c}$$
$$I_4(m_{\tilde{q}},m_q,m_\chi)=\int_0^1 dx\frac{x^3(1-x)^2}{D^3}$$
$$=\frac{1}{2m_\chi^6}\left[\ln\frac{m_{\tilde{q}}^2}{m_q^2}-(m_{\tilde{q}}^2-m_q^2-m_\chi^4)L\right]-\frac{1}{m_{\tilde{q}}^2m_\chi^2}$$
$$-\frac{m_q^2(m_{\tilde{q}}^2-m_q^2-m_\chi^2)}{m_\chi^4\Delta}L+\frac{1}{\Delta}\left[\frac{m_q^2}{m_\chi^4}-\frac{1}{m_{\tilde{q}}^2}\left[1-\frac{m_q^2}{m_\chi^2}\right]^2+\frac{1}{2m_\chi^2}\right]$$
$$+\frac{3m_q^2}{\Delta^2}\left\{1+\frac{m_{\tilde{q}}^2-m_q^2}{m_\chi^2}+\left[\frac{m_q^2(m_{\tilde{q}}^2-m_q^2)}{m_\chi^2}-2m_q^2-m_{\tilde{q}}^2-m_\chi^2\right]L\right\}, \tag{B1d}$$
$$I_5(m_{\tilde{q}},m_q,m_\chi)=\int_0^1 dx\frac{x(1-x)(2-x)}{D^2}$$
$$=\frac{1}{2m_\chi^4}\left[\ln\frac{m_{\tilde{q}}^2}{m_q^2}-(m_{\tilde{q}}^2-m_\chi^2-m_q^2)L\right]$$
$$-\frac{1}{\Delta}\left\{L\left[2(m_{\tilde{q}}^2-m_\chi^2)+3m_q^2+\frac{m_q^2(m_{\tilde{q}}^2-m_q^2)}{m_\chi^2}\right]-3+\frac{m_q^2-m_{\tilde{q}}^2}{m_\chi^2}\right\}. \tag{B1e}$$

Here we have introduced the quantities

$$D=x^2m_\chi^2+x(m_{\tilde{q}}^2-m_q^2-m_\chi^2)+m_q^2, \tag{B2a}$$
$$\Delta=2m_\chi^2(m_q^2+m_{\tilde{q}}^2)-m_\chi^4-(m_{\tilde{q}}^2-m_q^2)^2, \tag{B2b}$$
$$L=\frac{2}{\sqrt{|\Delta|}}\arctan\frac{\sqrt{|\Delta|}}{m_q^2+m_{\tilde{q}}^2-m_\chi^2},\quad \Delta\geq 0,$$
$$=\frac{1}{\sqrt{|\Delta|}}\ln\frac{m_q^2+m_{\tilde{q}}^2-m_\chi^2+\sqrt{|\Delta|}}{m_q^2+m_{\tilde{q}}^2-m_\chi^2-\sqrt{|\Delta|}},\quad \Delta\leq 0. \tag{B2c}$$

Equations (B1) are only valid of $m_{\tilde{q}}>m_\chi$, which is always true in our case. Note also that I_{1-5} are finite as either $m_\chi\to 0$ or $\Delta\to 0$. The first case can be treated numerically in a straightforward fashion. The limit $\Delta\to 0$ can be treated by expanding Eqs. (B1) and (B2) around the point $m_\chi=|m_{\tilde{q}}-m_q|$. Alternatively, this limit can be treated numerically by setting Δ to some (small) constant δ as $\Delta\to 0$ and taking $m_\chi^2=m_q^2+m_{\tilde{q}}^2-\sqrt{4m_q^2m_{\tilde{q}}^2-\delta}$.

[1] E. W. Kolb and M. S. Turner, *The Early Universe* (Addison-Wesley, Reading, MA, 1990).

[2] For reviews, see H. P. Nilles, Phys. Rep. **110**, 1 (1984); H. E. Haber and G. L. Kane, *ibid.* **117**, 75 (1985); P. Nath, R. Arnowitt, and A. Chamseddine, *Applied N=1 Supergravity* (World Scientific, Singapore, 1984).

[3] E. Witten, Nucl. Phys. **B188**, 513 (1981); N. Sakai, Z. Phys. C **11**, 153 (1981); S. Dimopoulos and H. Georgi, Nucl. Phys. **B193**, 150 (1981).

[4] E. Gildener and S. Weinberg, Phys. Rev. D **13**, 3333 (1976); E. Gildener, *ibid.* **14**, 1667 (1976).

[5] U. Amaldi, W. de Boer, and H. Fürstenau, Phys. Lett. B **260**, 447 (1991); P. Langacker and M. Luo, Phys. Rev. D **44**, 817 (1991); J. Ellis, S. Kelley, and D. V. Nanopoulos, Phys. Lett. B **260**, 131 (1991).

[6] T. K. Hemmick *et al.*, Phys. Rev. D **41**, 2074 (1990).

[7] Early papers are H. Goldberg, Phys. Rev. Lett. **50**, 1419 (1983); J. Ellis, J. Hagelin, D. V. Nanopoulos, and M. Srednicki, Phys. Lett. **127B**, 233 (1983); J. Ellis, J. Hagelin, D. V. Nanopoulos, K. Olive, and M. Srednicki, Nucl. Phys. **B238**, 453 (1984). Some recent examples are K. Griest, M. Kamionkowski, and M. S. Turner, Phys. Rev. D **41**, 3565 (1990); K. Olive and M. Srednicki, Nucl. Phys. **B355**, 208 (1991); M. M. Nojiri, Phys. Lett. B **261**, 76 (1991); J. L. Lopez, D. V. Nanopoulos, and K. Yuan, Nucl. Phys. **B370**, 445 (1992); J. Ellis and L. Roszkowski, Phys. Lett. B **283**, 252 (1992); P. Nath and R. Arnowitt, Phys. Rev. Lett. **70**, 3696 (1993).

[8] D. O. Caldwell *et al.*, Phys. Rev. Lett. **61**, 510 (1988); **65**, 1305 (1990); C. Bacci *et al.*, Phys. Lett. B **293**, 460 (1992); **295**, 330 (1992).

[9] Kamiokande Collaboration, M. Mori *et al.*, Phys. Lett. B

270, 89 (1991); **289**, 463 (1992).
[10] M. W. Goodman and E. Witten, Phys. Rev. D **31**, 3059 (1985).
[11] J. Ellis and R. A. Flores, Nucl. Phys. **B307**, 883 (1988).
[12] K. Griest, Phys. Rev. Lett. **62**, 666 (1988); Phys. Rev. D **38**, 2357 (1988).
[13] M. Srednicki and R. Watkins, Phys. Lett. B **225**, 140 (1989).
[14] G. F. Giudice and E. Roulet, Nucl. Phys. **B316**, 429 (1989).
[15] M. A. Shifman, A. I. Vainshtein, and V. I. Zakharov, Phys. Lett. **78B**, 443 (1978).
[16] M. Drees and M. M. Nojiri, Phys. Rev. D **47**, 4226 (1993).
[17] For reviews, see, e.g., H. D. Politzer, Phys. Rep. C **14**, 129 (1974); A. J. Buras, Rev. Mod. Phys. **52**, 199 (1980); E. Reya, Phys. Rep. **69**, 195 (1981); G. Altarelli, *ibid.* **81**, 1 (1982).
[18] J. Ellis and R. A. Flores, Phys. Lett. B **263**, 259 (1991); **300**, 175 (1993).
[19] M. Kamionkowski, Phys. Rev. D **44**, 3021 (1991).
[20] J. Ellis and S. Rudaz, Phys. Lett. **128B**, 248 (1983).
[21] M. Drees and M. M. Nojiri, Nucl. Phys. **B369**, 54 (1992).
[22] M. Drees and M. M. Nojiri, Phys. Rev. D **47**, 376 (1993).
[23] G. B. Gelmini, P. Gondolo, and E. Roulet, Nucl. Phys. **B351**, 623 (1991).
[24] S. Mizuta and M. Yamaguchi, Phys. Lett. B **298**, 120 (1993).
[25] T. P. Cheng, Phys. Rev. D **38**, 2869 (1988); H.-Y. Cheng, Phys. Lett. B **219**, 347 (1989).
[26] F. Gabbiani and A. Masiero, Nucl. Phys. **B322**, 235 (1989).
[27] J. G. Morfin and W.-K. Tung, Z. Phys. C **52**, 13 (1991).
[28] J. F. Owens, Phys. Lett. B **266**, 126 (1991).
[29] T. Hatsuda and T. Kunihiro, Nucl. Phys. **B387**, 705 (1992).
[30] J. Gasser, H. Leutwyler, and M. E. Sainio, Phys. Lett. B **253**, 252 (1991).
[31] See, e.g., R. L. Jaffe and A. Manohar, Nucl. Phys. **B337**, 509 (1990), and references therein.
[32] SLAC–Yale Collaboration, G. Baum *et al.*, Phys. Rev. Lett. **51**, 1135 (1983).
[33] EMC, J. Ashman *et al.*, Nucl. Phys. **B328**, 1 (1989).
[34] SMC Collaboration, B. Adeva *et al.*, Phys. Lett. B **302**, 533 (1993); SLAC E142 Collaboration, P. L. Anthony *et al.*, SLAC Report No. PUB-6101, 1993 (unpublished).
[35] J. Ellis and M. Karliner, CERN Report No. TH-6898/93 (unpublished).
[36] Y. Okada, M. Yamaguchi, and T. Yanagida, Prog. Theor. Phys. **85**, 1 (1991); H. E. Haber and R. Hempfling, Phys. Rev. Lett. **66**, 1815 (1991); R. Barbieri, M. Frigeni, and F. Caravaglio, Phys. Lett. B **258**, 395 (1991); J. Ellis, G. Ridolfi, and F. Zwirner, *ibid.* **262**, 477 (1991); M. Drees and M. M. Nojiri, Phys. Rev. D **45**, 2482 (1992).
[37] T. Shutt *et al.*, IEEE Trans. Nucl. Sci. **NS-37**, 547 (1990); Phys. Rev. Lett. **69**, 3425 (1992).
[38] J. Gould, Astrophys. J. **321**, 571 (1987).
[39] J. Engel, S. Pittel, and P. Vogel, Int. J. Mod. Phys. E **1**, 1 (1992).
[40] For example, ALEPH Collaboration, D. Decamp *et al.*, Phys. Rep. **216**, 253 (1992); L3 Collaboration, O. Adriani *et al.*, CERN Report No. PPE-93-31 (unpublished), and references therein.
[41] A. Bottino, V. de Alfaro, N. Fornengo, A. Morales, J. Puimbedon, and S. Scopel, Mod. Phys. Lett. A **7**, 733 (1992).
[42] For a review, see L. E. Ibàñez and G. G. Ross, in Perspectives in Higgs Physics, edited by G. L. Kane (unpublished).
[43] M. Drees, Int. J. Mod. Phys. A **4**, 3635 (1989); G. L. Kane, C. Kolda, and J. D. Wells, Phys. Rev. Lett. **70**, 2686 (1993); D. Comelli and C. Verzegnassi, Phys. Rev. D **47**, 764 (1993); U. Ellwanger, Phys. Lett. B **303**, 271 (1993).
[44] M. S. Turner, Phys. Rev. D **33**, 889 (1986); R. A. Flores, Phys. Lett. B **215**, 73 (1988).
[45] J. F. Gunion and H. E. Haber, Nucl. Phys. **B272**, 1 (1986).